Master's Thesis

석사 학위논문

Development of a New Single Port Surgery Robot

with Increased Torque and Workspace

Byungsik Cheon (천 병 식 千 昞 植)

Department of Robotics Engineering

로봇 공학 전공

DGIST

2013

Master's Thesis
석사 학위논문

Development of a New Single Port Surgery Robot
with Increased Torque and Workspace

Byungsik Cheon (천 병 식 千 昞 植)

Department of Robotics Engineering

로봇 공학 전공

DGIST

2013

Development of a New Single Port Surgery Robot with Increased Torque and Workspace

Advisor : Professor Jaesung Hong

Co-advisor : Professor Jeonil Moon

Co-advisor : Professor Pyunghoon Jang

by

Name
Department of Robotics Engineering
DGIST

A thesis submitted to the faculty of DGIST in partial fulfillment of the requirements for the degree of Master of Robotics Engineering. The study was conducted in accordance with Code of Research Ethics[1]

1. 3. 2012

Approved by

Professor Jaesung Hong (　　　)
(Advisor)

Professor Jeonil Moon (　　　)
(Co-Advisor)

---

[1] Declaration of Ethical Conduct in Research: I, as a graduate student of DGIST, hereby declare that I have not committed any acts that may damage the credibility of my research. These include, but are not limited to: falsification, thesis written by someone else, distortion of research findings or plagiarism. I affirm that my thesis contains honest conclusions based on my own careful research under the guidance of my thesis advisor.

Development of a New Single Port Surgery Robot

with Increased Torque and Workspace

Byungsik Cheon

Accepted in partial fulfillment of the requirements for the degree of Master of
Robotics Engineering.

12. 3. 2013

Head of Committee   Professor Jaesung Hong

Committee Member   Professor Jeonil Moon

Committee Member   Professor Pyunghoon Jang

ABSTRACT

This paper presents the development of a new single port surgery robot, <u>P</u>lat spring driven mechanism equipped robot for single port <u>LA</u>paroscopic <u>S</u>urgery (PLAS), with plate spring driven mechanism.

Recently, the number of single port laparoscopic surgery (SILS) that can easily conceal postoperative scars is increasing, and robotic SILS platforms are being developed for solving inconvenient maneuverability of manual SILS. However, the drive mechanism of most robotic SILS platforms existing consists of wire, therefore cannot afford to deliver sufficient force, and the wire is mechanically deformed, thus causing negative effects on movement accuracy. Due to this limitation, a precious operation cannot be conducted by using conventional robotic SILS platforms. Accuracy and force are reduced as the workspace is expanding. The purpose of proposed robot is to increase tissue handling force of forceps by using plate spring driven mechanism, and to conduct more stable and precious operations in an expanded area. Evaluations of PLAS were performed and its feasibility as a new effective robotic SILS platform was proved

Keywords: Plate spring driven mechanism, SILS, laparoscopic surgery, robotic SILS platform,

Contents

List of contents

List of tables

List of figures

I. INTRODUCTION

1.1 Introduction to Single Incision Laparoscopic Surgery (SILS)

Medical technology of modern world has been increasingly advanced with help of engineering. For example, developments of camera technology enable surgeons to build laparoscopic surgeries in which they can observe diseased spots by inserting a laparoscope through a tiny hole and conduct operations with laparoscopic forceps. Unlike traditional open surgery, laparoscopic surgery is an operation in which three or four tiny holes with 10~15mm are made in abdominal area, and the abdominal cavity is inflated by injecting carbon dioxide, and therein, a laparoscope and other medical instruments are put in for an operation. Benefits of this method are that postoperative scars are small enough, compared with an open surgery, which results in enhanced cosmesis, and that the period of recovery is shorter and postoperative pain is much less for patients. Moreover, complications and sequelas along with operations are much under control [1].

Constant efforts to reduce incisions size in operations have been made. Transition is made from initial open surgery to laparoscopic surgery, which is now widely used for operations. And the concern

with NOTES and SILS as the next generation of laparoscopic surgery has been growing. NOTES is a non-invasive surgery, where either stomach or large intestine is perforated after a robot is inserted through either mouth or anal passage of patients, after which a diseased area is approached. However, there are several problems to solve, so some of difficulties are had in clinical trials [2, 3, 4]. Compared to this, SILS is a feasible operating method [5, 6], using specialized instruments, and particularly for the case of SILS using navel, it is getting popular for minimizing incision area.

The first single port surgery was reported by Esposito C [7]. In 1998, and initial SILS had technical limits because traditional laparoscopic instruments were used. Yet, constant research has been ongoing, and instruments for SILS as Shown on figure 1, 2 [8], and as a result, it was considered as a substitute for conventional laparoscopic surgery [5, 6].

Figure 1. HiQ LS Curved Ø 5 mm Hand Instruments,   http://www.olympus-global.com

Figure 2. SILS™ Hand InstrumentsSILS™, http://www.covidien.com/

Rapidly spread is SILS where an operation is conducted with the only one port instead of three to four ports. SILS is an operation in which an incision with the size of 15~20mm around the navel is made and abdominal cavity is inflated with CO_2 and then laparoscope and medical instruments are inserted together for the operation. A postoperative scar is invisible since this operation is conducted in a navel area, which is natural orifice of the body [9], and the convalescence is short. Not conducting open surgery also reduces the stress of patients that might come along with the operation, from which immune system is less damaged [1]. Therefore, this operation is getting popular for people who are interested in body appearance and for parents with children who are going to have surgery. This operating technique is evolving into other different operations. For now, the possible operations with SILS are cholecystectomy, appendectomy, hysterectomy, tubal ligation, ovarian cystectomy, nephrectomy, partial nephrectomy[10], ureterolithotomy [11], prostatectomy, and especially widely used in gynecology.

However, surgeons are reluctant to conduct SILS because it has some technical challenges. One of the biggest problems of SILS is counter-intuitive operation, which might happen because operations are conducted by the only one port with forceps intersected like 'X', where Surgeon might have confusing sense of direction for left and right hand. A great deal of training is needed to overcome confusing sense of direction, and also a high level concentration and longtime are required for surgeon to conduct operations without medical instruments' physically crashed each other [12, 13, 14]. In addition, surgeon's visibility is likely to decrease because laparoscope and other medical instruments are located in one line [1]. Due to this problem, Surgeons have difficulties securing clear view and manipulating surgical instruments.

To breakthrough this obstacle, a lot of manual instruments such as figure 1 and 2 for SILS have been developed to overcome these problems but the result was so far not effective. A simple example for this is pre articulated forceps of Olympus. However, this product is not available for high level operations due to its limited workspace.

1.2 Previous researches of robotic SILS

There were efforts to solve problems of SILS with robots. Robotic SILS can easily solve the problem of the counter-intuitive operation and quickly and easily conduct delicate surgery with precise control, in most cases. However, these efforts face difficulties in being developed owing to structural limits that force should be delivered through small-sized-port. Despite this obstacle, researches are preceding in several labs in that the usage of robot system is more feasible for operators to easily conduct the surgery, solving problem of robotic SILS.
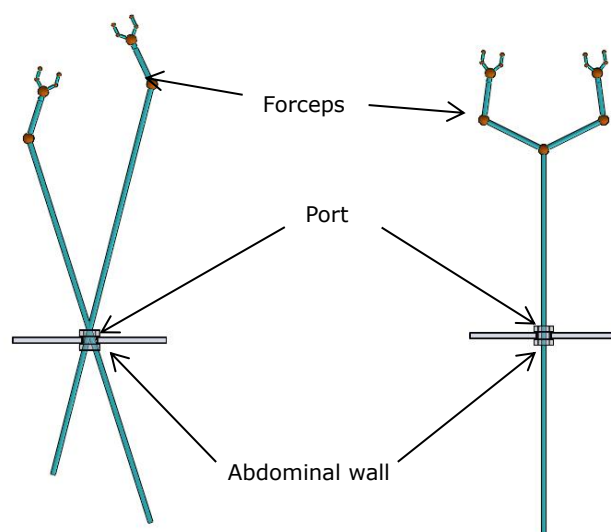
Figure 3. Type of robotic SILS platform; X-type (left), Y-type (right)

The types of Robotic SILS are divided into X and Y type. Robotic SILS of X type is to use motorized laparoscopic forceps such as when using laparoscopic forceps for SILS with intersection. This type

also makes same triangulation making the counter intuitive problem of SILS, but it has a slave system

which is a controller switched left and right [15]. The examples of X type are using da Vinci and da Vinci

S not Si [12] and a master-slave robot system for SILS developed by Dr. Yuki Horise (Osaka University,

Japan) [16]. X-type SILS robot has enough force to conduct operation. However, these kinds of robots oc-

casionally has external collisions between arms while conducting operations because da Vinci surgical

system is originally developed for multiport laparoscopic surgery so it has too long and big arms to con-

duct SILS [12]. Another disadvantage is its bulky hardware size because a laparoscope and two forceps

devices should be attached to three serial robots, which is like da Vinci robots. This weakness cannot be

easily ignored concerning operating robots. Operating room needs the minimization of medical devices in

size-wise since the room is already full of complex devices. This weakness also leads to inconvenience

when converting to open surgery in an emergency situation while conducting operations. While X type

robot has an intersected structure with each laparoscopic forceps, Y-type SILS robot has two state which

are 'I' and 'Y'. Its initial state is 'I' for insertion to one small incision such as figure 4. After insertion, two

forceps are spread to 'Y' shape from 'I' shape, and thereby easily control tissues without collisions be-

tween forceps. In this type, minimization is available because a laparoscope and two forceps don't have to

be attached to three serial robots, and manipulation is highly secured compared to the X-type robots.
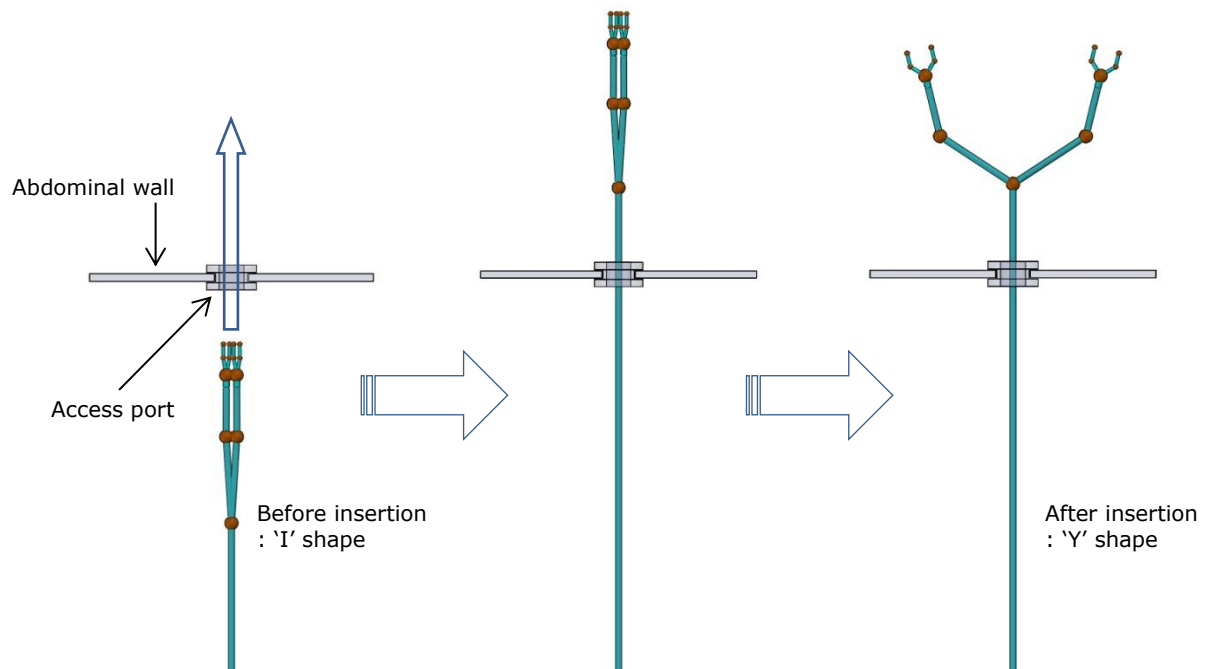
Figure 4. Folded state for insertion and unfolded state after insertion of Y-type SILS robot

Among Y-type SILS robots are SPIDER surgical system (TransEnterix, Morrisville, NC, USA), IREP(Columbia University New York, US) and SPRINT(Scuola Superiore Sant'Anna, Pisa, Italy), etc, which is considered to be an ideal SILS platform.

1.3 Advantages and disadvantages of current SILS robots

A representative of SILS robot is a SPIDER used in clinical trial after getting approved by FDA [17]. SPIDER surgical system has a substantially small size and is easy to learn because of its simple control. Forceps needed is inserted to flexible channel and moved, and then the wire connected to handles is

given tension, which makes the edge of forceps move as wanted. Moreover, the exchange of operating in-struments is rapidly conducted through two flexible channels, and necessary medical aids such as suction tubes and camera can be inserted through two rigid ports. But, the convenience of manipulation is not good since it is a passive robot, and force-delivering-wire cannot fully support payloads for normal surgery, only limited range of operations such as gastric band and gastric sleeve surgeries are possible, not taking too much load.

Figure 5. SPIDER® Surgical System, www.transenterix.com

IREP developed in Colombia University is a snake-like continuum robot with 14 degrees of free-dom [18]. Its movement is quite sophisticated, and can afford the operation where it can be inserted through between ribs as well as navel since it is one of the slimmest in size among Y type SILS robots. Moreover, surgeons feel perspective during the operations, because 3D camera is attached. However, its speed is slow and force (2 N) is weak in conducting general operation [18].

SPRINT being developed in Pisa University in Italy shows the strongest force among Y type SILS robots. This robot with 6 degrees of freedom in each arm does not use wires in delivering force unlike other operating robots. Also, Motors are included inside arm, and its force is stable because the force is directly delivered by mechanical gears [19]. The weakness of this robot is that the diameter of an arm is thick, since motors and gears are installed inside of robot's arm. Because of this reason, diameter of introducer such as trocars is 34mm [19], which is relatively large to use is for clinical operations. In an upgraded version of this robot, minimization is said to be available because of minimized gear, using CNC technique. However, when using this robot with electrosurgery, it might have electric shock Hazards in patients during an operation, since electric wires for motors are place inside of the arm and its electric insulation can be easily damaged at articulated and rotational joints.

Other examples of SILS robots are Stackable 4-BAR Manipulators for SILS [20] and a SILS robot using Flexible Shaft being developed which can bring out substantial force without using wires [21, 22], but have limited manipulation and limited degrees of freedom, needed for an operation.

1.4 Plate spring driven mechanism.

The biggest problem based on the analysis of SILS is that its volume is small and it doesn't have appropriate force delivering device that should deliver force for the operation. Volume of drive mechanism and force are trade-off relationship, so the bigger force become, the larger the volume of mechanism gets. The smaller volume of drive mechanism becomes, the more reduced the output force become. Mechanical gear and wires can be taken as examples. Gear can deliver a big force using gear ratio, but its size is large, which leads to expanding the volume of arms of robots. Wires ($\emptyset$ 0.2~0.8mm) that can be used in activating operation robots have small volume in its size, but its stiffness is so low that it cannot deliver enough force. In order to decide on effective force delivering device, it is important to build up an appropriate mechanism that can contribute to appropriate size and force based on trade-off relationship. In this study plate spring driven mechanism satisfying this condition was developed, and a principle of plate spring driven mechanism is as following.

Plate spring can afford to deliver tension such as wires. Yet, in case that compression is added, compressive force is absorbed to elasticity energy due to buckling, and thus it is not able to deliver the force to the end of the opposite side. In this situation, if a guide preventing buckling in both sides of spring

is installed such as figure 6, compressive force does not become absorbed to elastic energy and therefore

plate spring comes to deliver the compressive force. Hence, plate spring driven mechanism can deliver not

only tension unlike wires but compressive force at the same time shown in figure 8. Also, since it does not

need a structure for rewinding like wires, simple structure is provided, and the more force can be delivered

as cross sectional area is widened. Moreover, plate spring driven mechanism only needs a guide while pul-

ley should be established in a curve area in a wire operation.
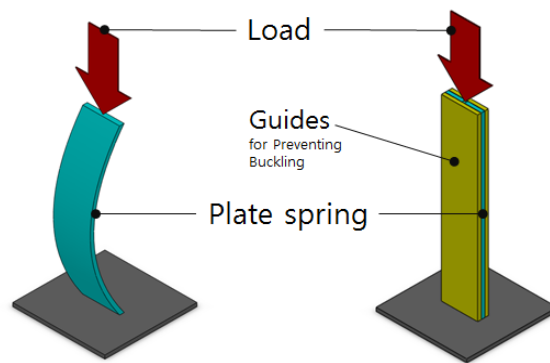
Figure 6. An example of buckling and preventing buckling
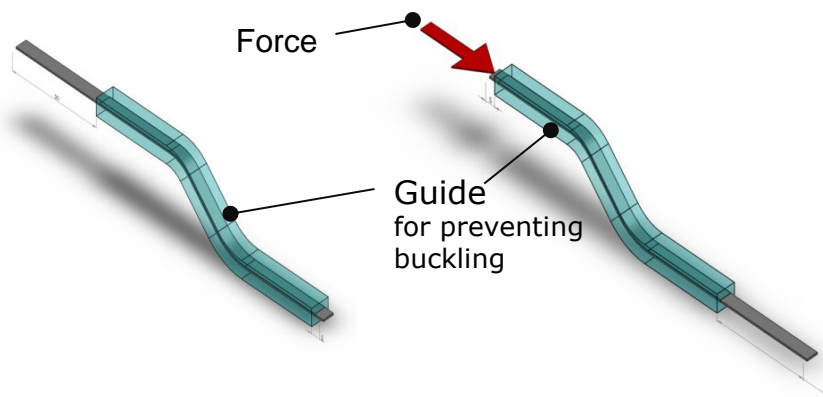
Figure 7. Concept of plate spring driven mechanism
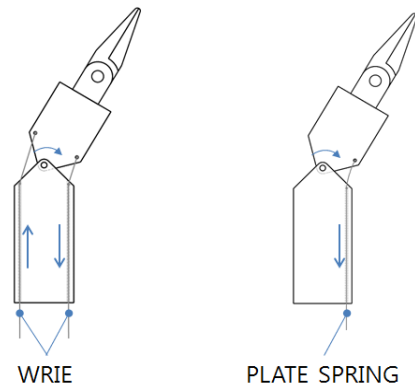
Figure 8. Comparison of wire & plate spring driven mechanism
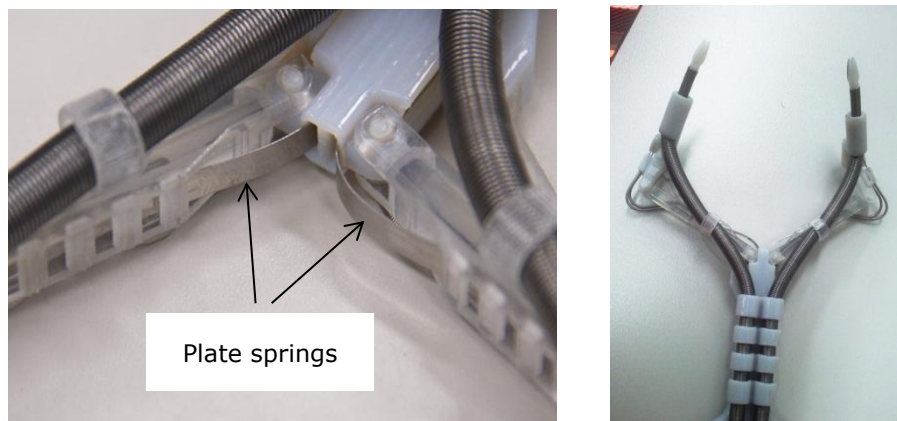
Plate springs

Figure 9. Example of applying plate spring driven mechanism at PLAS

The weakness of this mechanism is as following. When plate spring is passing a curve area, if a radius of rotation in a curve is so small, resistance severely takes place, and plate spring causes plastic deformation. Continuously repeated weight in this situation raises the change of surface structure of deformed spot, thus bringing out fatigue fracture. And, lubrication and elaborate surface processing of guides and plate spring are needed in order to minimize the friction because spring contacts with a surface of guides which are to hinder buckling. In this study, plate spring driven mechanism is applied to only one joint needing most torque, and the

joint and form installed are well explained in the next mechanism chapter.

1.5 Research contents and goals

In this study, a more effective robotic SILS platform is meant to be manufactured, adopting strong points and solving weaknesses based on the considerations of currently developed SILS robots [15]. One of the most important factors in developing operating robots needs not only engineering approach for performance but also a deep understanding of body in medical view. First, requests and opinions of surgeon who would use surgical robots should be actively accepted. Second, Errors coming from misunderstanding in developing robots should be prevented by easily explaining technical parts to doctors so that they can be well understood. In order to develop robots suggested in this study, a close look about SILS is taken, and the amounts of payloads needed for operations are measured. Next, strong and weak points of existing SILS robots are assessed and common problems are taken into account. Afterwards, concepts, overcoming these problems are devised and applied to a robot design, adding opinions of surgeons. As a solution, principles and advantages of plate spring mechanism designed in this study are described, and the utility of plate spring mechanism is verified, assessing performance of SILS robot.

The goal of this study lies in developing a surgical robot platform that can effectively conduct single

port surgeries based on a deep understanding of SILS and cooperation with surgeons and the purpose of this

study is increasing a performance, stabilizing operations through constant trials.

II. DESIGN

2.1 Ideal robotic SILS platform

To develop effective robotic SILS platform, the essential points of the ideal robotic SILS platform have been gathered by considering conventional and robotic SILS. First one is diameter of SILS robot's should be as small as much of 2~2.5cm in diameter of a tiny access port. However, in cases of SILS robots which have small diameter, actuators are installed at the back so as to minimize a diameter of robots, and forces are delivered to the end of forceps by passing devices such as wires. Wires can easily move though round areas such as joints because of its flexibility, but it stiffness not enough for surgical operations. As an example of da Vinci surgical system, the use of wire-driven-forceps is restricted to 10 ten times to secure accuracy of the robot. Secondly, they should have enough force, which is approximately 10N for operations. Usually, robots which have enough force are too big to be inserted in the umbilical access port because that these kinds of robots have mechanical gears, rigid links as drive mechanisms that may cause bulky size of SILS robots. Thirdly, an appropriate structure of SILS robot is Y shape to conduct single port surgeries to avoid collisions between arms. Fourthly, Y type SILS robots should have six degrees of freedom or more so that operations should be smoothly conducted. Its organization of six DOF is four DOF for

conventional laparoscopic forceps, one DOF which is needed to transform between 'I' shape for insertion and 'Y' shape for operation, and another one DOF of prismatic joint, specially devised in this study. Fifthly, during operations, many kinds of surgical instruments are needed so SILS robot should have a convenient structure to exchange instruments needed. Finally, safety design should be considered. For an example, manufacturing surgical robots with an actuator inside of its arms which is inserted to patients' body had better be avoided for electric safety. Particularly, risk of electronic hazard is getting increased in operations when going abreast with electro-surgery.

2.2 New robotic SILS platform
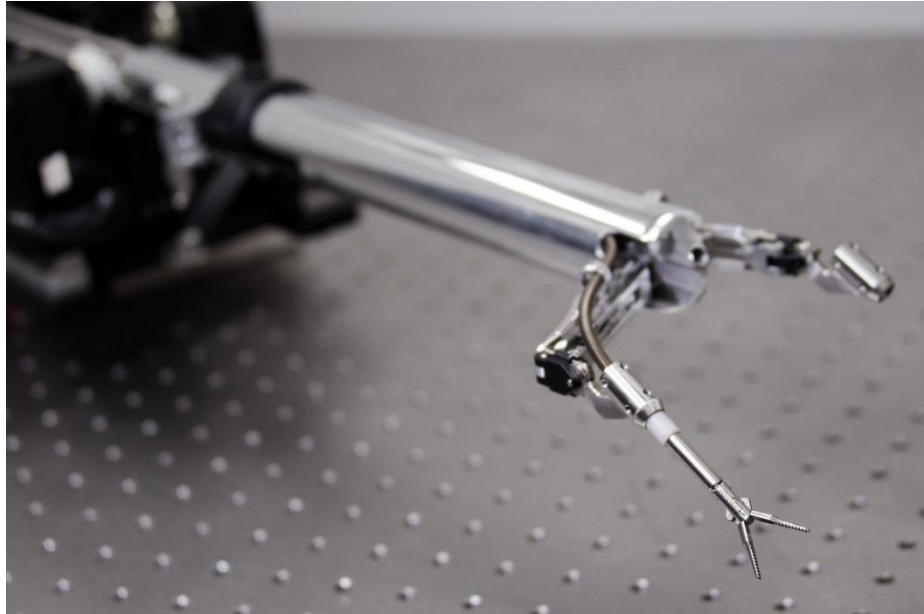
Figure 10. PLAS

An effective robotic SILS platform, PLAS (Plat spring driven mechanism equipped robot for single port LAparoscopic surgery), has been developed based on the ideal robotic SILS given above. I have tried to accommodate essential points of the ideal robotic SILS for development of the robot, but some points have not been accommodate. First one, the diameter (33mm) of PLAS's main stem is larger than ideal diameter (20~30mm) due to production costs. Originally, a body material of the proposed robot was stainless steel, but its processing cost was high. So, it was replaced by aluminum of which the processing cost is relatively low. However, since stiffness of the material property of aluminum is not strong enough to be applied to its initial design, a length of diameter of main stem expands to Ø 33mm.   33mm-length of

main stem is relatively thick as SILS platform, but real bodies are not used in this study, and the length of

diameter of SPINT developed by a leading group of this field is also 34mm [19]. And because proving the

efficiency of plate spring driven mechanism is a more important goal, modification of design was tried.

Second, wires were used in order to activate tilting joint. At first, the usage of wire was not deeply consid-

ered to deliver a strong force, but wires are used so as to reduce manufacture cost. Third, it is not designed

to be a structure where medical instruments can be replaced. The reason is to reduce the cost of instru-

ments and the tool was made fixed. Besides, conditions of ideal SILS platform mentioned previously were

applied to platform.

2.1.1   Force requirement

C. Richards et al. report that the force range of tool-tip is ±20N while dissecting the gallbladder

fossae during laparoscopic cholecystectomy [23]. M. Lazeroms et al. suggested that ±10N is required for

laparoscopic surgery [24]. But, any conventional robotic SILS platforms don't have as much force as nec-

essary. Only SPRINT equipped with mechanical gears could take as much as 5N [19]. IREP which has

wire driven mechanism could handle less than 2 N [18]. The force range of SPIDER surgery system

equipped with wire driven mechanism has not been reported yet, but every operational maneuver per-

formed with difficulty because of a lack of strength [17]. Although the FDA approved SPIDER surgery

system but it is rarely used. To handle more strong force, currently developed robotic SILS platforms

adopt gears and screw while avoiding wires [19, 22]. In PLAS case, plate spring driven mechanism is

adopted to handle sufficient force. In this paper, force requirement is 10N.

2.1.2　Considerations on work space and degree of freedom

In deciding on the range of operation and the length of arms, following process was referred. Ex-

pressed are the size of inside of abdominal cavity and every organ that are insufflated by CO2, using 3D

modeling program so that it can cover every single operation. The anatomical size of the inside of ab-

dominal cavity insufflated depends on the amount of CO_2 injected. The size of a body is modeled accord-

ing to the size of an average body of adults such as figure 11, and the amount of CO_2 injected is decided to

$3000cm^3$ that is average amount in laparoscopic operation such as figure 11. A length of main stem is decid-

ed based on the access to every abdominal organ after inserting robot imitation to the spot of navel of modeled

body such as figure 9. The length of the arm is also decided to the size where each abdominal organ is effec-
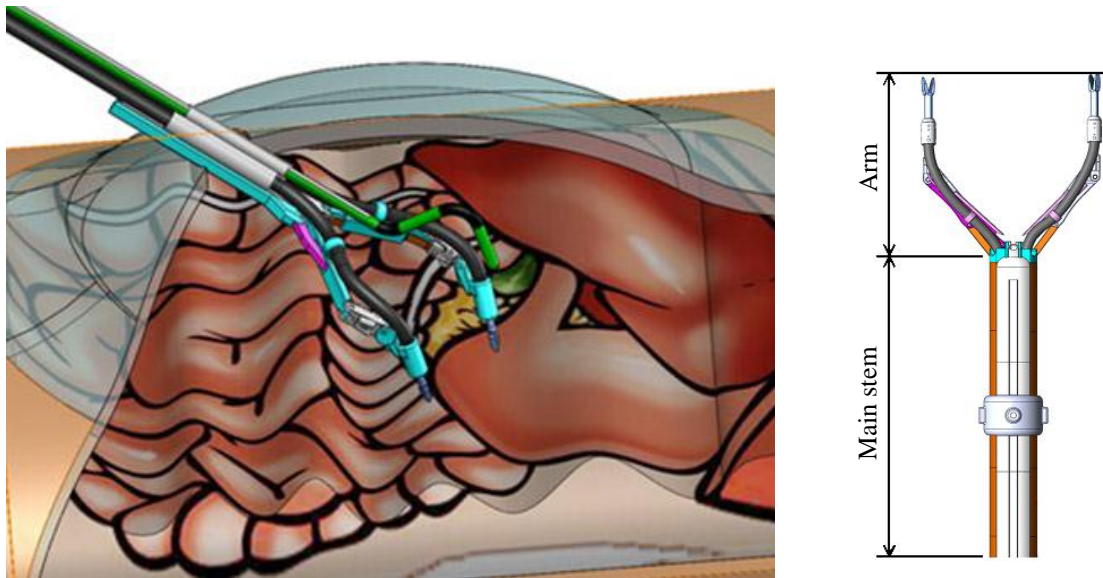
tively caught.
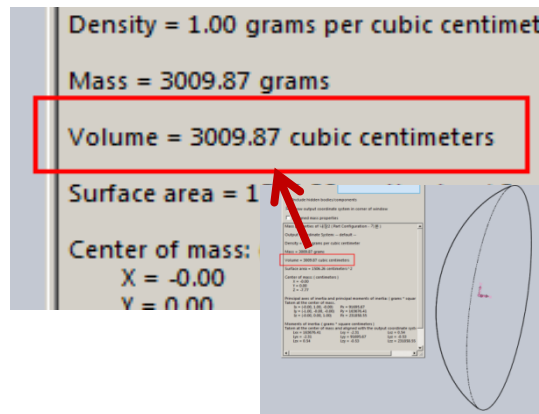
Figure 11. Volume of CO_2 for SILS
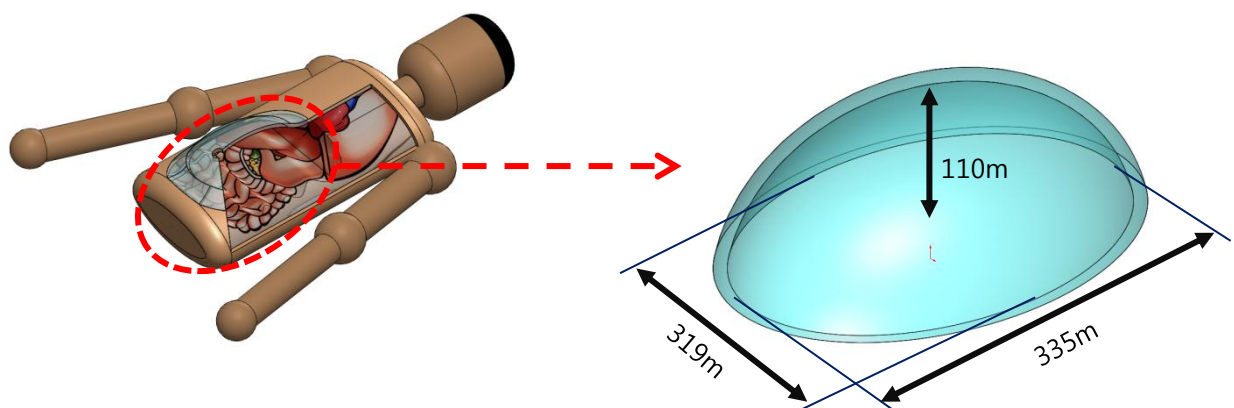
Figure 12. Modeling of abdominal cavity

Figure 13. Length decision of arm and main stem

PLAS is dual arm robot with six DOF per arm. The structure is as following. It consists of 4 DOF

of general manual forceps shown on figure 14, 1 DOF needed when the Y-type robot is folded to 'I' shape,

and 1 DOF of prismatic joint, specially devised for proposed robotic SILS platform such as figure 15.
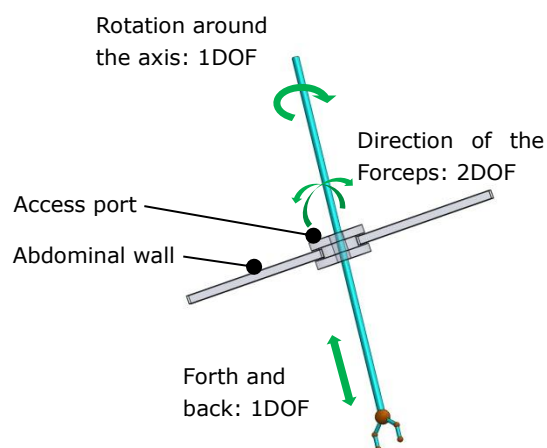
Figure 14. Normal Forceps have 4DOF

Usually, Y-type SILS robots are not appropriate in dealing with relatively large organs such as

liver, intestine in that the starting point of two arms is fixed differently from manual SILS and X-type

SILS robots which have a long stroke between the end of the laparoscopic forceps. In order to solve this

problem, long stroke is secured with separating the starting point of two arms of Y-type robot and in-

stalling the long prismatic joint shown in figure 15.
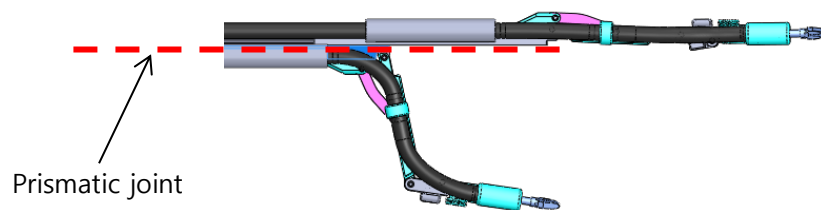
Figure 15. Y-type SILS robot with an additioinal prismatic joint
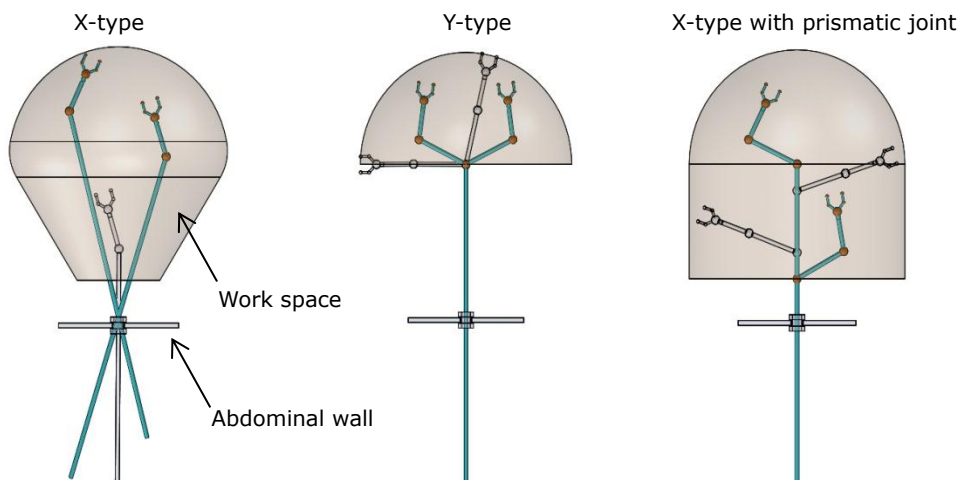
Figure 16. Comparison of work space according to robot's type

2.3 Mechanical implementation of joints

Proposed robot platform developed through this study are divided to two parts: one is a surgery part, conducting operations, with being inserted to the body of patients, and the other is an actuation part, delivering forces to the surgery part such as figure 17. The surgery part consists of a main stem and two arms for operation.
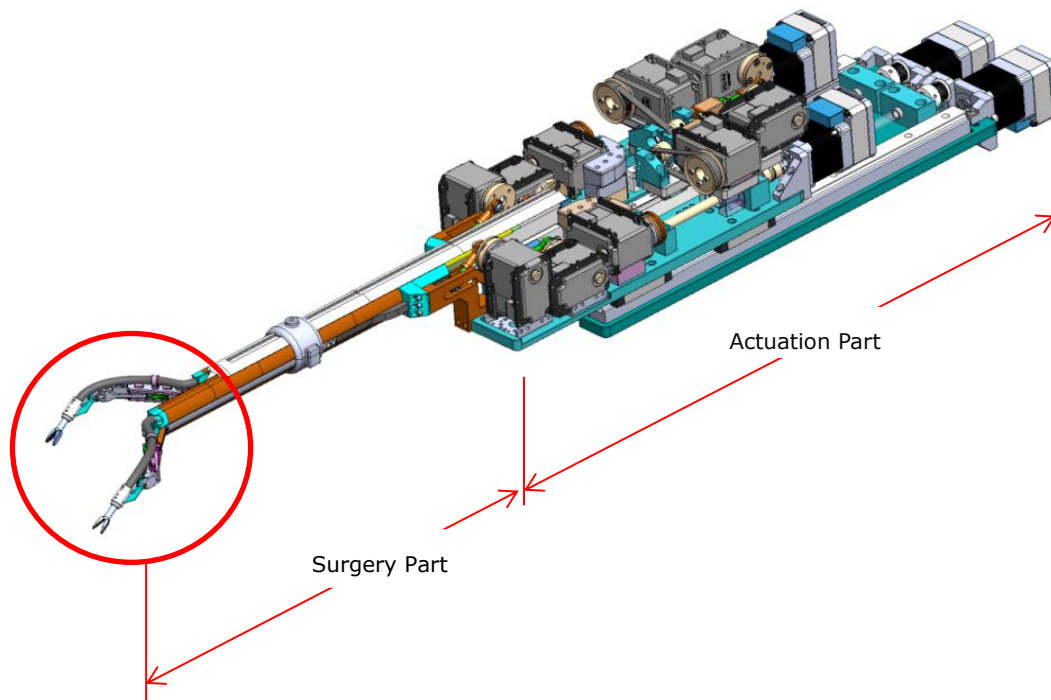
Figure 17. The structure of SILS robot, Surgery part and Actuation part
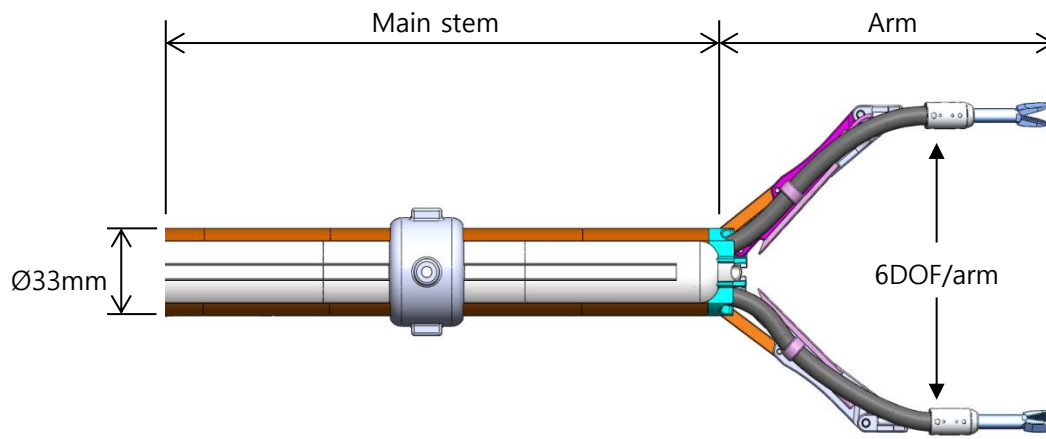
Figure 18. The main stem and arms of surgery part.

The cylindrical main stem is passage of the plate springs and wires that deliver forces from actuation parts to arms. Outer shape is designed in a circle shape in order to be compatible with trocars which are introducers for the subsequent placement of surgical instruments without CO_2 leak such as figure 19.
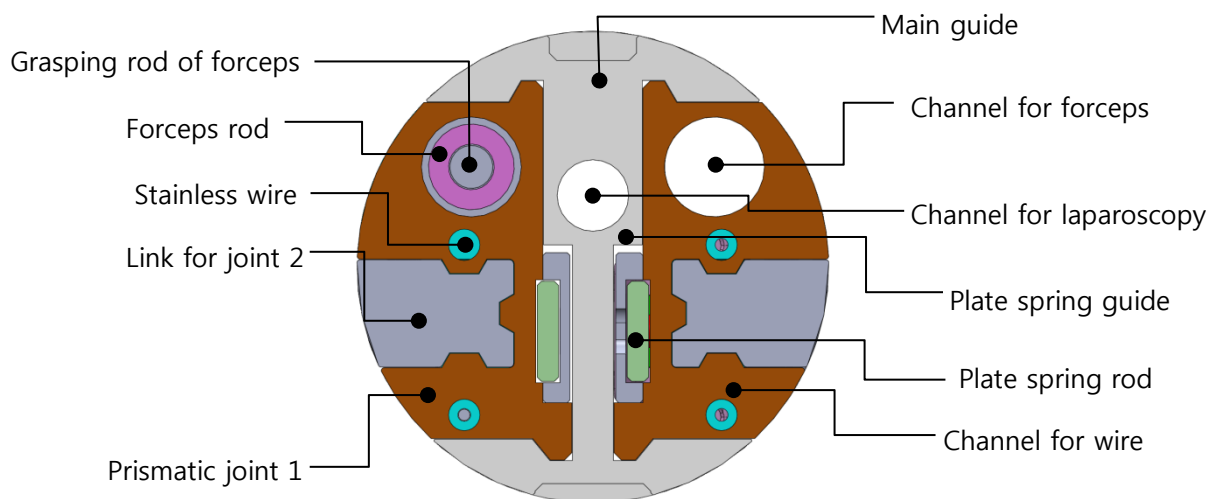
Figure 19. Cross-section diagram of the main stem

Each arm of the surgery part has 6 DOF and one gripper, and each motor which controls each joint is as shown on figure 20.
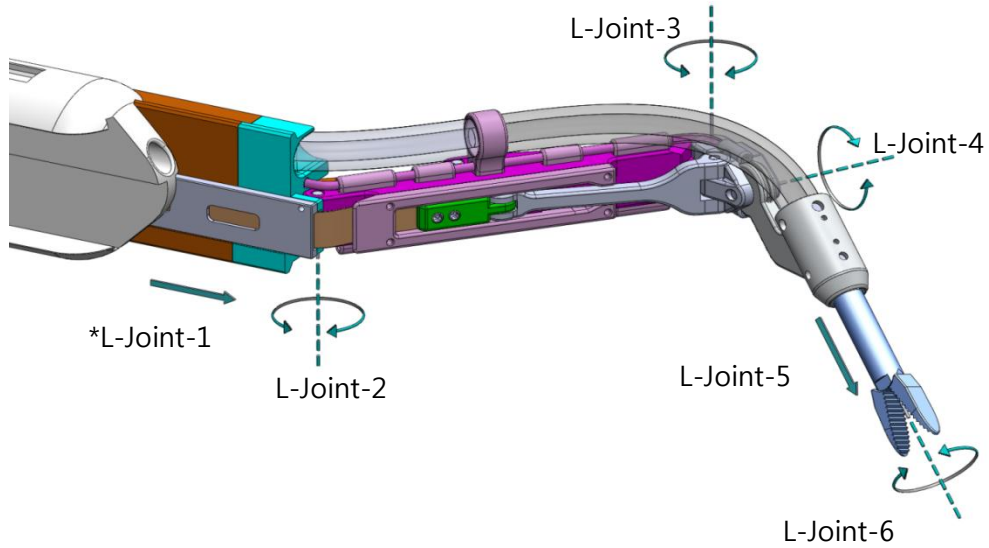
Figure 20. A structure of degrees of freedom, *L: left
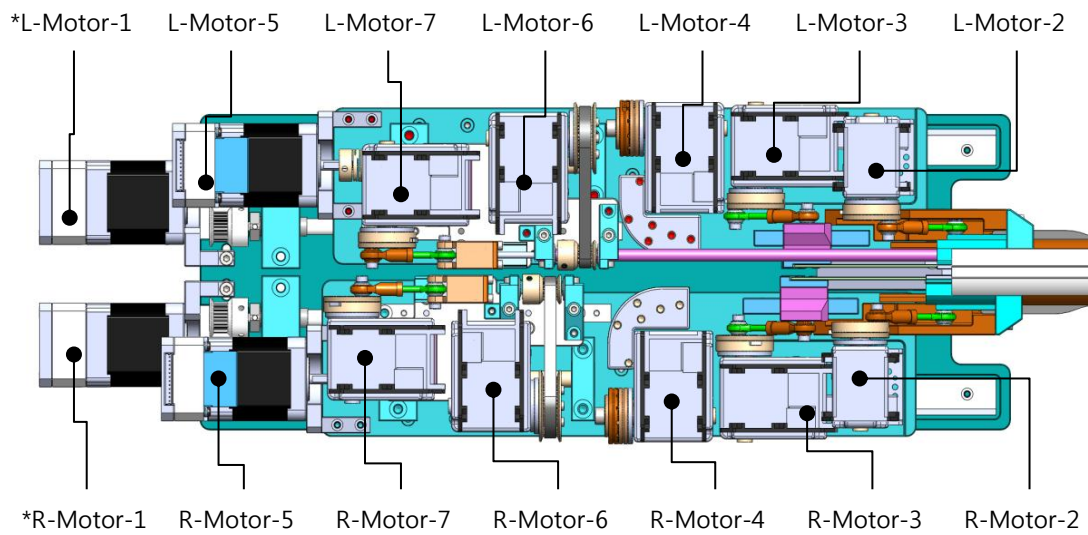
Figure 21. Motors of the actuation part, *L: left, *R: right

Table 1. Relation of joints and motors

Joint *i*	connected Motor *i*
L-Joint-1	L-Motor-1
L-Joint-2	L-Motor-2
L-Joint-3	L-Motor-3
L-Joint-4	L-Motor-4
L-Joint-5	L-Motor-5
L-Joint-6	L-Motor-6
L-grasper joint	L-Motor-7
R-Joint-1	R-Motor-1
R-Joint-2	R-Motor-2
R-Joint-3	R-Motor-3
R-Joint-4	R-Motor-4
R-Joint-5	R-Motor-5
R-Joint-6	R-Motor-6
R-Grasper joint	R-Motor-7

Stepping L-Motor-1 activates prismatic Joint-1, playing a role of making the whole arm advance like a below Figure 22. When stepping L-Motor-1 is doing backlashing, a timing belt transmits this rotating movement to ball screw, which makes the whole arm move forward. Then, a linear guide is used in order to secure linearity. The maximum stroke of prismatic Joint-1 is 215mm.
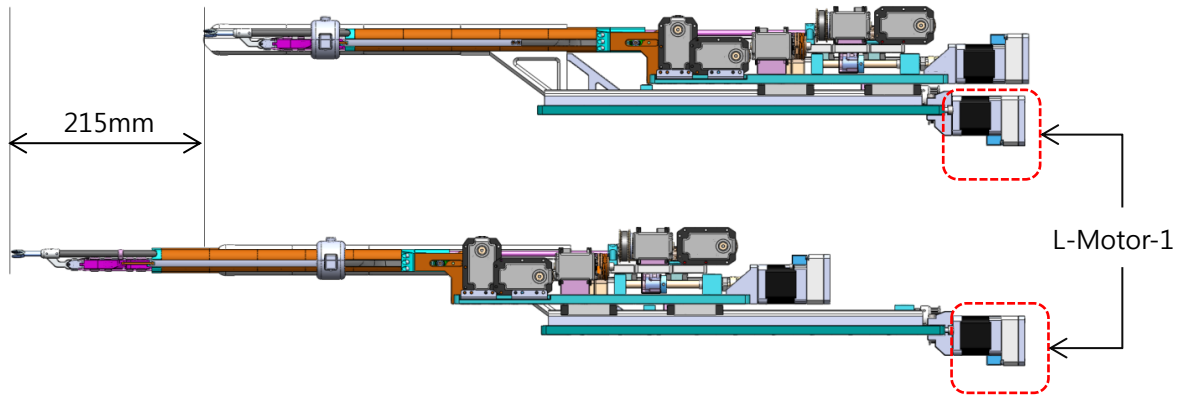
Figure 22. Prismatic Joint 1 stroke moved by stepping L-Motor 1
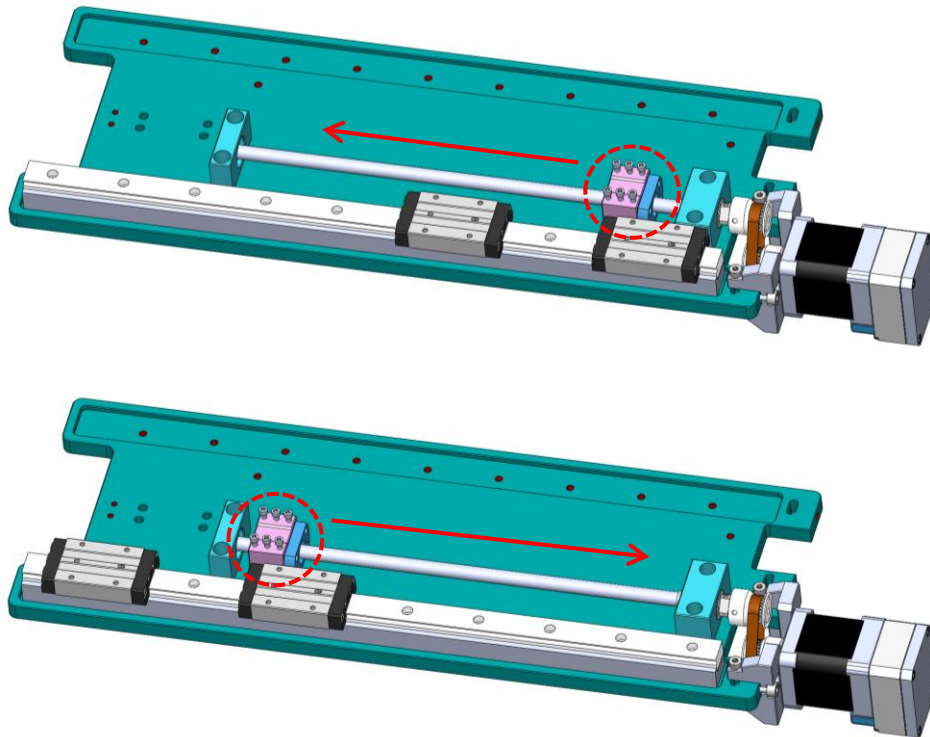
Figure 23. Ball screw, activating stepping L-Motor-1 and LM guide, securing linearity

Servo L-Motor-2 motivates rotational Joint--2, playing a role of folding and spreading arms

shown as figure 24. The process of movement is as followings. When L-Motor-2 is doing CW rotation, crank

pushes slider advance, and a link connected to slider pushes a lever, and forceps becomes parallel. As a

contrast, when L-Motor-2 is doing CCW rotation, the arm is unfolding such as figure 26. At this point, the

maximum spread angle is 80 degrees.
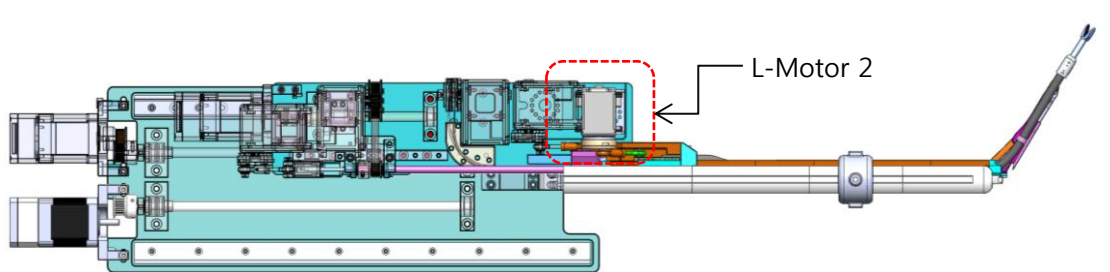
Figure 24. The position of L-Motor-2 and rotational Joint-2
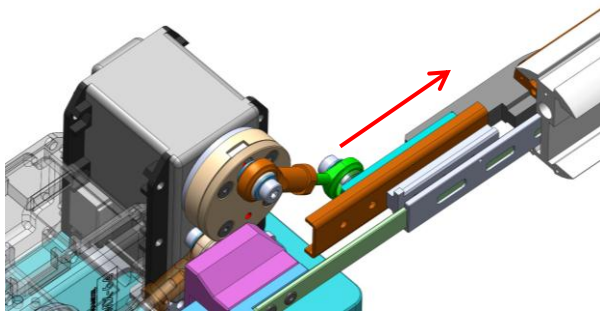
Figure 25. CCW rotation of L-Motor-2
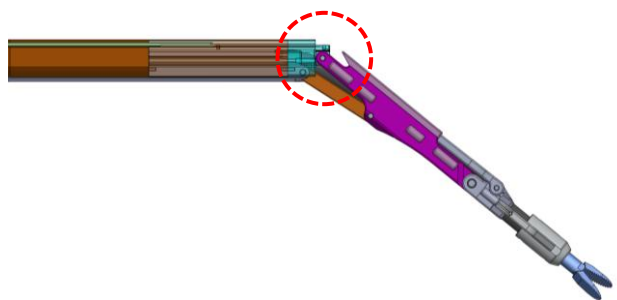
Figure 26. Unfolding state of arm by CCW rotation of

L-Motor-2
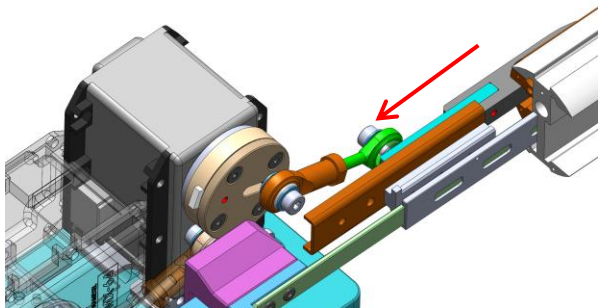
Figure 27. CW rotation of L-Motor-2
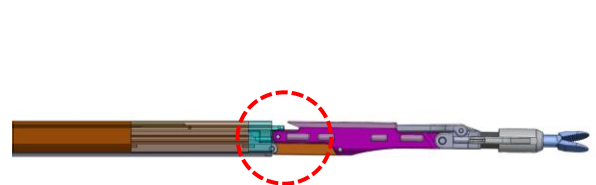
Figure 28. Folding state of arm by CW rotation of L-

Motor-2

Servo L-Motor--3 activates rotational Joint-3, and decides on the Yaw direction movement of

forceps. Order of operation is as following. When L-Motor-3 is rotating to a direction of CW, it pulls

spring and come to pull lever-2 connected to joint-3 shown in figure 30. Therefore, forceps become folded

such as figure 30. When L-Motor-3 is rotating to a direction CCW, forceps are unfolded shown as figure

31. At this point, the maximum spread angle is 110 degrees.
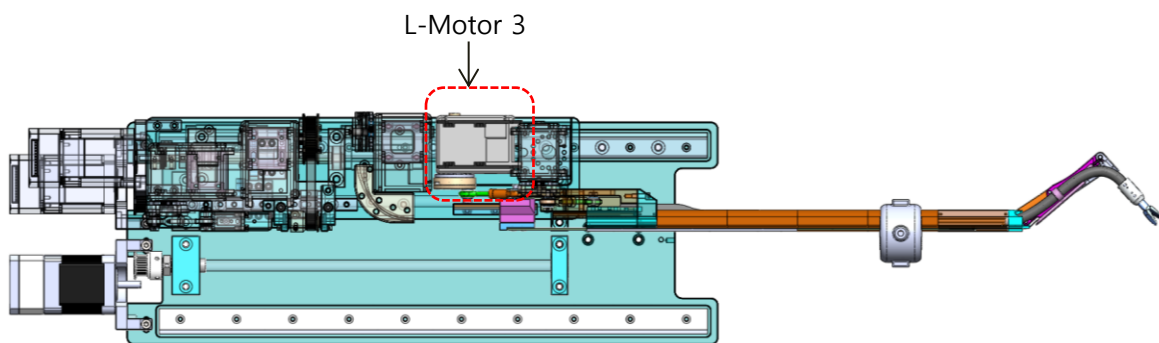
Figure 29. Position of L-Motor 3 and rotational L-Joint 3
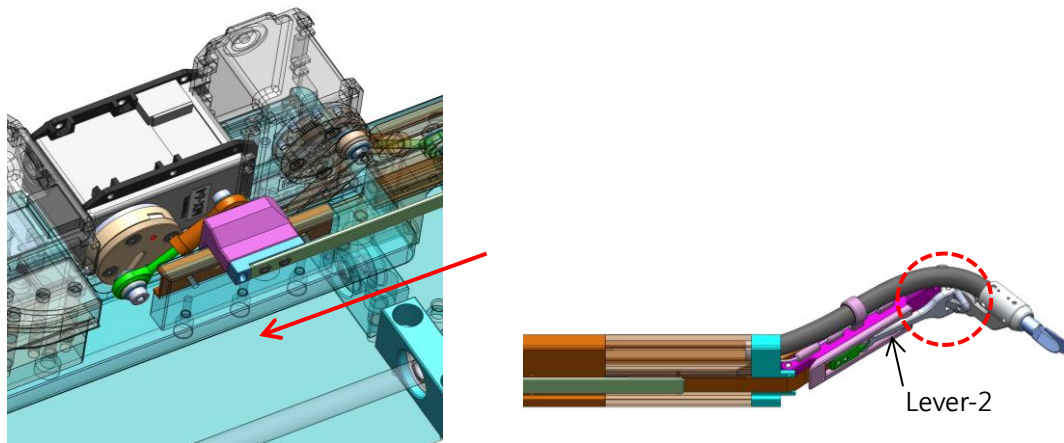
Figure 30. CW rotation of L-Motor-3 and folding of forceps
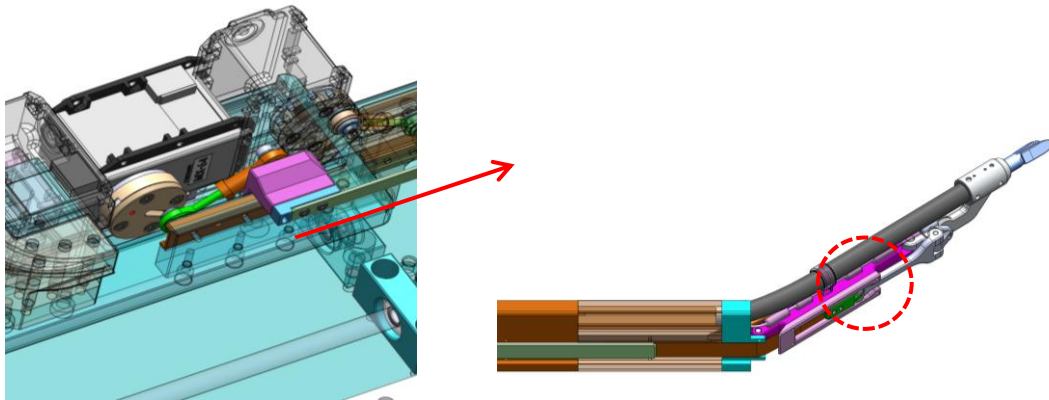
Figure 31. CCW rotation of L-Motor-3 and unfolding of forceps

L-Motor-4 initiates rotational Joint-4, and the process is such as figure 32. If L-Motor-4 is rotating to a direction of CCW, connected wires pull up over forceps. As a contrast, when L-Motor-4 rotates to a direction of CW, rotating forceps are moving downwards. At this point, degrees of tilting is ±45°
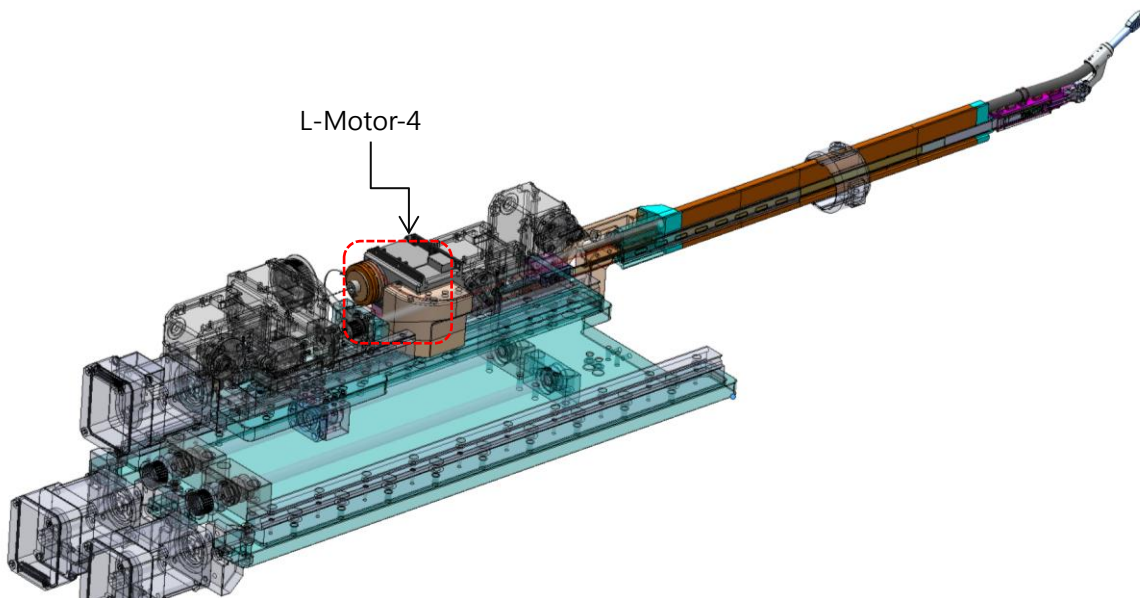
Figure 32. Position of L-Motor-4 and rotational Joint-4
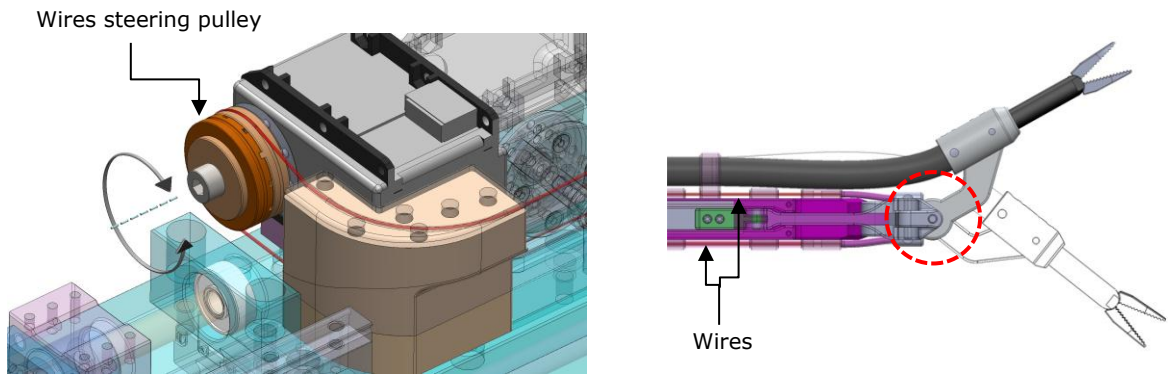
Figure 33. An example of L-Motor-4 and rotational Joint-4 tilting

L-Motor 5 activates prismatic Joint-5, playing a role of moving forceps forwards and backwards.

A principle of activation is as below. When L-Motor-5 is rotating CCW, it spins a ball screw connected to

flexible coupling, moving forceps forwards as the ball screw converts rotation movement to a straight line

motion. When L-Motor-5 is doing CW rotation, as a contrast, forceps move backwards. At this point, the

maximum stroke is 35mm.
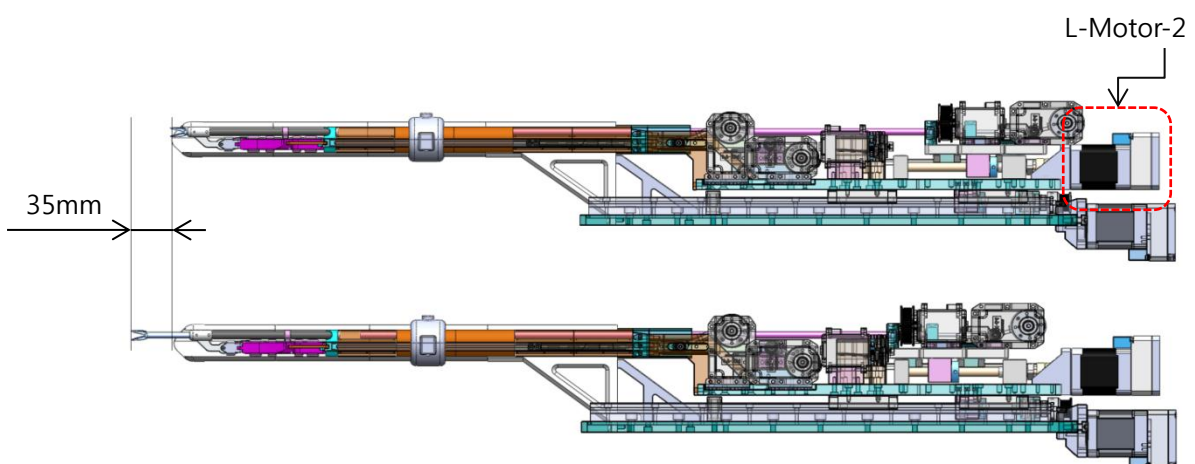
Figure 34. Position of L-Motor-5 and amounts of stoke of prismatic Joint-5
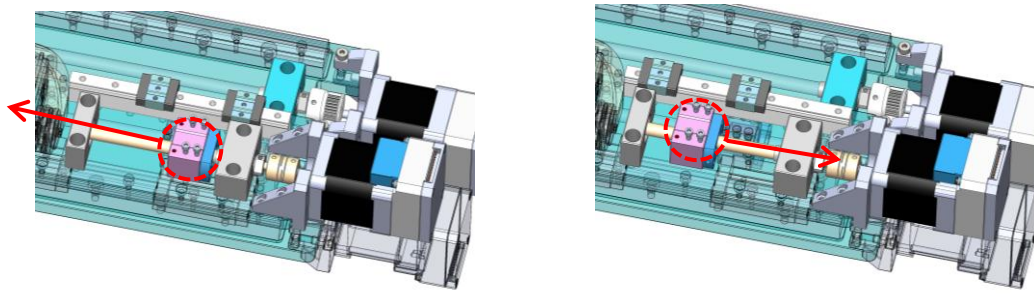
Figure 35. The ball screw activated by L-Motor-3, and LM guide securing linear motion.

L-Motor-6 activates rotational Joint-6, playing a role of rotating forceps. Order of control is as following. When L-Motor-6 rotates, timing belt rotates, leading to a rotation of rod and then, forceps.
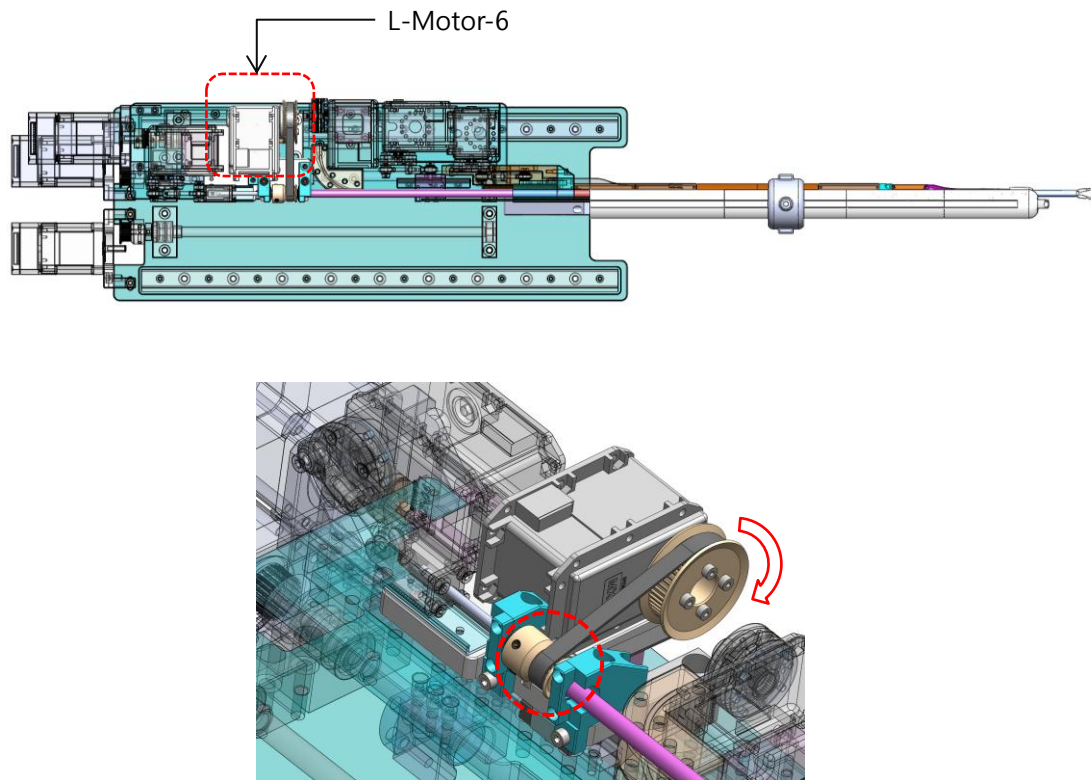
Figure 36. Position of L-Motor-6 and connected mechanism
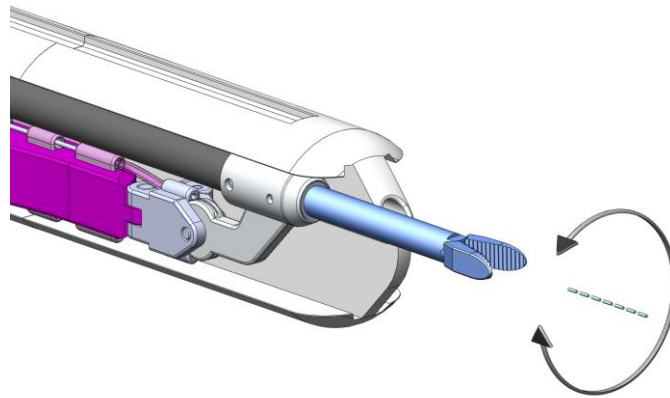
Figure 37. Rotational joint-6

L-Motor-7 activates the movement of forceps grasping. Order of movement is as following.

When L-Motor-7 rotates to a direction of CCW, connected crank push the LM guide, making gripper of forceps open. As a contrast, when motor rotates to a direction of CW, gripper of forceps gets closed.
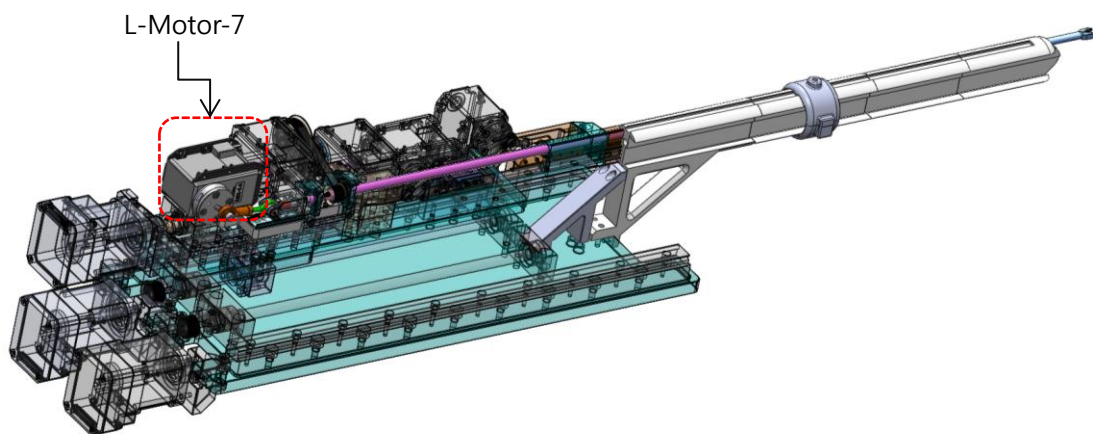
Figure 38. Position of L-Motor-7
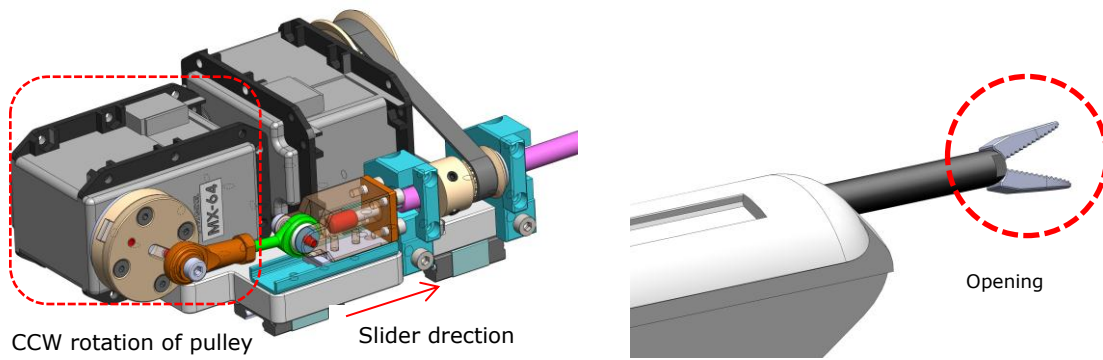
Figure 39. Opening of forceps by counter-rotation of L-Motor-7
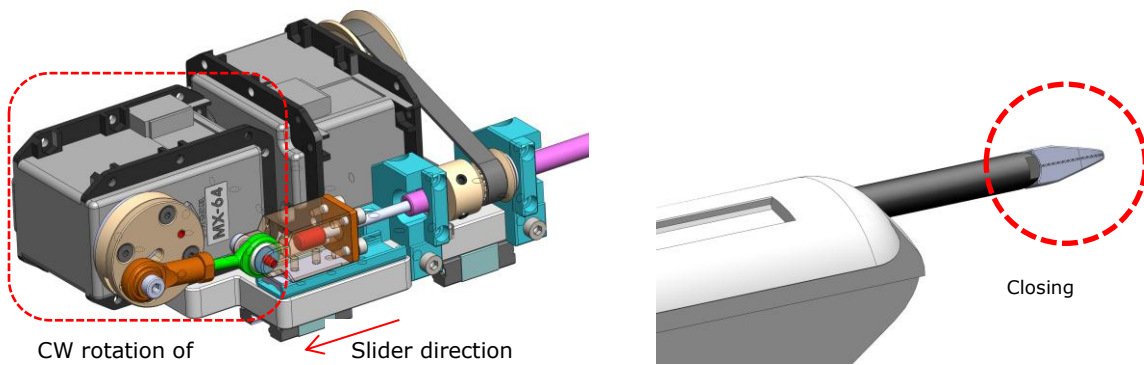
Figure 40. Closing of forceps by normal-rotation of L-Motor-7

In controlling forceps grasping, proper controlling of force is necessary since excessive grasping

force could contribute to damages of internal organs of patients. However, since a sensor that can detect

feedback on generated force is not available in this robot, designed and applied is a device that can absorb

unnecessary force and adjust torque of motors. When L-Motor-7 rotating CCW, pulling rod pusher in-

stalled in LM guide, elastic block is pulled back, and as an elastic block absorbs the force, grasping force

can properly decline.
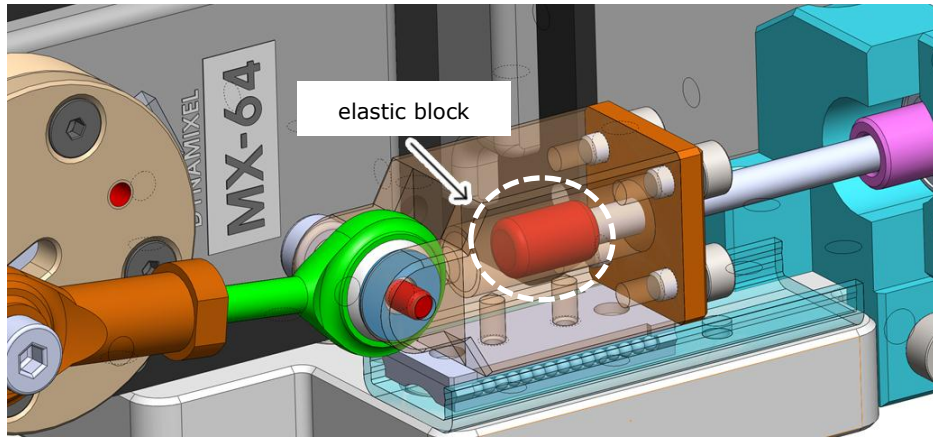
Figure 41. An applied example of a elastic block

III. DIRECT AND INVERSE POSITION ANALYSIS

Although the original manipulator that is designed for the single port surgery in this study employs closed loop linkages to drive the second and the third joints of each arm, throughout this section it will be treated as two distinct 6-DoF serial manipulators and only one arm will be analyzed. The treatment will not affect the results as the closed loop linkages in the design are simply transferring the motions of the actuators located away from the system to the joints and they have no effect on the kinematics of the manipulator. Also it should be noted that the fifth and the sixth joints represents the linear and the rotational motion of the forceps that will be inserted into the system.

Kinematic representation of the left arm of the system is shown in figure 42, and its axes are labeled with respect to the distal Denavit - Hartenberg convention. The corresponding Denavit - Hartenberg parameters are also tabulated in Table 2 In addition, the workspace of the proposed robot is calculated and shown as figure 43.

The transformation matrix between the i_{th} and the $(i-1)_{th}$ coordinate system can be obtained by translating $(i-1)_{th}$ coordinate system along the z_{i-1} axis by d_i, rotating the resulting system around z_{i-1} axis by θ_i, translating resulting system along the x_i axis by a_i, and finally rotating the resulting system around x_i axis by α_i, (1).
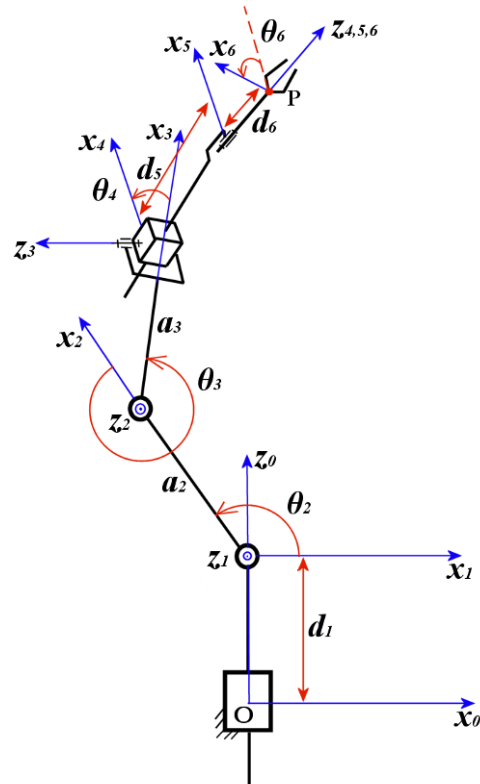
Figure 42. Kinematic representation of 6-DoF serial

manipulator
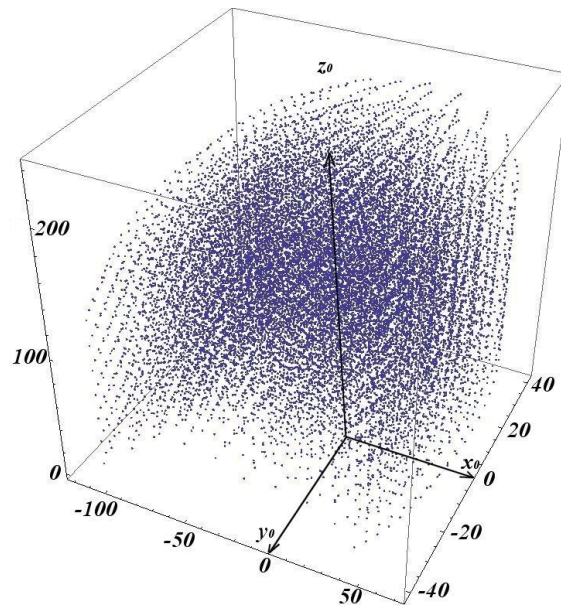
Figure 43. The workspace of an arm

Table 2. D-H parameters of the serial manipulator

Joint i	α_i	a_i	d_i	θ_i
1	$\pi/2$	0	d_1 = variable	0
2	0	a_2	0	θ_2 = variable
3	$3\pi/2$	a_3	0	θ_3 = variable
4	$\pi/2$	0	0	θ_4 = variable
5	0	0	d_5= variable	0
6	0	0	d_6	θ_6 = variable

$$^{i-1}T_i = T(z_{i-1},d_i)T(z_{i-1},\theta_i)T(x_i,a_i)T(x_i,\alpha_i)$$

(1)

where,

$$T(z_{i-1},d_i) = \begin{bmatrix} 1 & 0 & 0 & 0 \\ 0 & 1 & 0 & 0 \\ 0 & 0 & 1 & d_i \\ 0 & 0 & 0 & 1 \end{bmatrix}, \quad T(z_{i-1},\theta_i) = \begin{bmatrix} C_i & -S_i & 0 & 0 \\ S_i & C_i & 0 & 0 \\ 0 & 0 & 1 & 0 \\ 0 & 0 & 0 & 1 \end{bmatrix},$$

$$T(x_i,a_i) = \begin{bmatrix} 1 & 0 & 0 & a_i \\ 0 & 1 & 0 & 0 \\ 0 & 0 & 1 & 0 \\ 0 & 0 & 0 & 1 \end{bmatrix}, \quad T(x_i,\alpha_i) = \begin{bmatrix} 1 & 0 & 0 & 0 \\ 0 & C\alpha_i & -S\alpha_i & 0 \\ 0 & S\alpha_i & C\alpha_i & 0 \\ 0 & 0 & 0 & 1 \end{bmatrix}$$

and $C_i = \cos\theta_i$, $S_i = \sin\theta_i$, $C\alpha_i = \cos\alpha_i$, and $S\alpha_i = \sin\alpha_i$. Multiplying the matrices in order with re-

spect to the (1) $^{i-1}T_i$ can be expanded as,

$$
{}^{i-1}T_i = \begin{bmatrix} C_i & -C\alpha_i S_i & S\alpha_i S_i & a_i C_i \\ S_i & C\alpha_i C_i & -S\alpha_i C_i & a_i S_i \\ 0 & S\alpha_i & C\alpha_i & d_i \\ 0 & 0 & 0 & 1 \end{bmatrix}
\tag{2}
$$

In order to calculate the final transformation matrix ${}^{0}T_6$ between the floating coordinate system of the end effector and the fixed ground global coordinate system of the manipulator, series of matrix multiplications should be carried out.

$$
{}^{0}T_6 = {}^{0}T_1 \, {}^{1}T_2 \, {}^{2}T_3 \, {}^{3}T_4 \, {}^{4}T_5 \, {}^{5}T_6
\tag{3}
$$

Substituting the D-H parameters in Table 1 to (2) and using (3) ${}^{0}T_6$ will be calculated as,

$$
{}^{0}T_6 = \begin{bmatrix} u_x & v_x & w_x & p_x \\ u_y & v_y & w_y & p_y \\ u_z & v_z & w_z & p_z \\ 0 & 0 & 0 & 1 \end{bmatrix}
\tag{4}
$$

where,

$u_x = C_{23} C_4 C_6 - S_{23} S_6$, $u_y = C_6 S_4$, $u_z = S_{23} C_4 C_6 + C_{23} S_6$,

$v_x = -S_{23} C_6 - C_{23} S_6 C_4$, $v_y = -S_6 S_4$, $v_z = -S_{23} C_4 S_6 + C_{23} C_6$, $w_x = C_{23} S_4$, $w_y = -C_4$, $w_z = S_{23} S_4$,

$p_x = a_2 C_2 + C_{23}(a_3 + S_4(d_5 + d_6))$, $p_y = -C_4(d_5 + d_6)$, $p_z = a_2 S_2 + d_1 + S_{23}(a_3 + S_4(d_5 + d_6))$

where, $C_{ij} = \cos(\theta_i + \theta_j)$, and $S_{ij} = \sin(\theta_i + \theta_j)$.

3.1 Direct Kinematics

The objective of the direct kinematics is to find the manipulator end effector location that includes both position and orientation by giving the values of the joint angles for revolute pairs and the joint translation amounts for prismatic pairs. Any position vector represented in end effector coordinate system

$^6q = [^6q_x, ^6q_y, ^6q_z, 1]^T$ can be expressed in the fixed ground global coordinate system

$^0q = [^0q_x, ^0q_y, ^0q_z, 1]^T$ by using the transformation matrix $^0T_6$ in the formulation,

$$^0q = {}^0T_6 \, {}^6q \tag{5}$$

As the point p is the origin of the end effector coordinate system $^6p = [0,0,0,1]^T$, the end effector position expressed in the fixed ground global coordinate system will be the last column of the transformation matrix $^0T_6$, $^0p = [p_x, p_y, p_z, 1]^T$. Also the orientation of the end effector can be represented by the three unit vectors (u_x, u_y, u_z), (v_x, v_y, v_z) and (w_x, w_y, w_z) as they form the rotation matrix inside the transformation matrix,

$$^0T_6 = \begin{bmatrix} [^0R_6]_{3x3} & [^0p]_{3x1} \\ [0]_{1x3} & 1 \end{bmatrix} \tag{6}$$

3.2 Inverse Kinematics

The objective of the inverse kinematics is to find the joint angles for revolute pairs and the joint translation amounts for prismatic pairs by giving the location of the end effector. As the values of the transformation matrix $^0T_6$ components are given, variable joint parameters $(d_1, \theta_2, \theta_3, \theta_4, d_5, \theta_6)$ can be calculated by using (4) as follows,

$$\frac{v_y}{u_y} = \frac{-S_6 S_4}{C_6 S_4} = -\tan \theta_6$$

$$\theta_6 = \tan^{-1}(-\frac{v_y}{u_y}) \tag{7}$$

$$w_y = -C_4, \; p_y = -C_4(d_5 + d_6)$$

$$d_5 = \frac{p_y}{w_y} - d_6 \tag{8}$$

As θ_6 is known from (7),

$$v_y = -S_6 S_4, \; w_y = -C_4$$

$$\frac{v_y}{S_6 w_y} = \tan \theta_4, \; \theta_4 = \tan^{-1}(\frac{v_y}{S_6 w_y}) \tag{9}$$

and,

$$\frac{w_z}{w_x} = \frac{S_{23} S_4}{C_{23} S_4} = \tan \theta_{23}$$

$$(\theta_2 + \theta_3) = \tan^{-1}(\frac{w_z}{w_x}) \tag{10}$$

In order to proceed further in the calculation of remaining variable parameters, (3) can be modified by pre and post multiplying it with $({}^{0}T_{1}\,{}^{1}T_{2})^{-1}$ and ${}^{5}T_{6}^{-1}$ respectively.

$$({}^{0}T_{1}\,{}^{1}T_{2})^{-1}\,{}^{0}T_{6}\,{}^{5}T_{6}^{-1} = {}^{2}T_{3}\,{}^{3}T_{4}\,{}^{4}T_{5} = {}^{2}T_{5} \tag{11}$$

here,

$$
{}^{2}T_{5} = \begin{bmatrix} C_3C_4 & -S_3 & C_3S_4 & C_3(a_3 + S_4d_5) \\ S_3C_4 & C_3 & S_3S_4 & S_3(a_3 + S_4d_5) \\ -S_4 & 0 & C_4 & C_4d_5 \\ 0 & 0 & 0 & 1 \end{bmatrix} \tag{12}
$$

and the left portion of the (11) results in,

$$
({}^{0}T_{1}\,{}^{1}T_{2})^{-1}\,{}^{0}T_{6}\,{}^{5}T_{6}^{-1} = \begin{bmatrix} l_x & m_x & n_x & r_x \\ l_y & m_y & n_y & r_y \\ l_z & m_z & n_z & r_z \\ 0 & 0 & 0 & 1 \end{bmatrix} \tag{13}
$$

where,

$l_x = C_6(C_2u_x + S_2u_z) - S_6(C_2v_x + S_2v_z)$, $\quad l_y = C_6(-S_2u_x + C_2u_z) + S_6(S_2v_x - C_2v_z)$, $\quad l_z = -C_6u_y + S_6v_y$,

$m_x = S_6(C_2u_x + S_2u_z) + C_6(C_2v_x + S_2v_z)$, $\quad m_y = -S_2(-S_6u_x + C_6v_x) + C_2(S_6u_z + C_6v_z)$, $\quad m_z = -S_6u_y - C_6v_y$,

$n_x = C_2w_x + S_2w_z$, $\quad n_y = -S_2w_x + C_2w_z$, $\quad n_z = -w_y$, $\quad r_x = -a_2 + C_2(p_x + d_6w_x) - S_2(d_1 - p_z + d_6w_z)$,

$r_y = S_2(-p_x + d_6w_x) - C_2(d_1 - p_z + d_6w_z)$, $\quad r_z = -p_y + d_6w_y$.

Equating (12) and (13),

$$\frac{n_x}{l_x} = \frac{C_3 S_4}{C_3 C_4} = \tan\theta_4$$

$$\frac{n_x}{l_x} = \frac{C_2 w_x + S_2 w_z}{C_6(C_2 u_x + S_2 u_z) - S_6(C_2 v_x + S_2 v_z)} \tag{14}$$

and using tangent half angle formulations in (14),

$$C_2 = \frac{1 - t_2^{\,2}}{1 + t_2^{\,2}}, \; S_2 = \frac{2t_2}{1 + t_2^{\,2}}, \; t_2 = \tan\frac{\theta_2}{2} \tag{5}$$

θ_2 can be solved as below,

$$\boldsymbol{\theta_2 = 2\tan^{-1} t_2} \tag{16}$$

where,

$$t_2 = \frac{k_1 \pm \sqrt{k_1^{\,2} + k_2^{\,2}}}{k_1} \quad ,$$

$$k_1 = w_z + (S_6 u_z - C_6 v_z)\tan\theta_4 \quad ,$$

$$k_2 = w_x + (S_6 v_x - C_6 u_x)\tan\theta_4$$

After the calculation of θ_2, θ_3 can be found by using (10),

$$\theta_3 = \tan^{-1}(\frac{w_z}{w_x}) - \theta_2 \tag{17}$$

and the last remaining parameter d_1 will be,

$$r_y = S_2(-p_x + d_6 w_x) - C_2(d_1 - p_z + d_6 w_z)$$

$$d_1 = \frac{S_2(-p_x + d_6 w_x) - r_y}{C_2} + p_z + d_6 w_z \tag{18}$$

It should be noted that there exist multiple solutions for the inverse kinematics problem. In order

to reduce the number of solutions, atan2 function can also be used where possible.

IV. VELOCITY AND JACOBIAN ANALYSIS

Velocity components of the end effector in the specified 6-DoF serial manipulator can be carried

out by using the actuated joint rates,

$$
\begin{bmatrix} v_6 \\ w_6 \end{bmatrix} = \mathbf{J} \begin{bmatrix} \dot{d}_1 \\ \dot{\theta}_2 \\ \dot{\theta}_3 \\ \dot{\theta}_4 \\ \dot{d}_5 \\ \dot{\theta}_6 \end{bmatrix} \tag{19}
$$

where, v_6 is the linear velocity of the origin of the end effector coordinate system,

$v_6 = \begin{bmatrix} v_{6x} & v_{6y} & v_{6z} \end{bmatrix}^T$, w_6 is the angular velocity of the end effector $w_6 = \begin{bmatrix} w_{6x} & w_{6y} & w_{6z} \end{bmatrix}^T$, and

$\mathbf{J}_{6x6}$ is a Jacobian matrix that transforms the actuated joint rates in the actuator space to the velocity state

in the end effector space.

The Jacobian matrix $\mathbf{J}$ can be subdivided in to $\mathbf{J}_1$ and $\mathbf{J}_2$, and (19) can be modified as,

$$
\begin{bmatrix} v_6 \\ w_6 \end{bmatrix} = \begin{bmatrix} \mathbf{J}_1 \\ \mathbf{J}_2 \end{bmatrix} \begin{bmatrix} \dot{d}_1 \\ \dot{\theta}_2 \\ \dot{\theta}_3 \\ \dot{\theta}_4 \\ \dot{d}_5 \\ \dot{\theta}_6 \end{bmatrix} \tag{20}
$$

where,

$$\mathbf{J}_1 = \begin{bmatrix} \dfrac{\partial p_x}{\partial d_1} & \dfrac{\partial p_x}{\partial \theta_2} & \dfrac{\partial p_x}{\partial \theta_3} & \dfrac{\partial p_x}{\partial \theta_4} & \dfrac{\partial p_x}{\partial d_5} & \dfrac{\partial p_x}{\partial \theta_6} \\[2mm] \dfrac{\partial p_y}{\partial d_1} & \dfrac{\partial p_y}{\partial \theta_2} & \dfrac{\partial p_y}{\partial \theta_3} & \dfrac{\partial p_y}{\partial \theta_4} & \dfrac{\partial p_y}{\partial d_5} & \dfrac{\partial p_y}{\partial \theta_6} \\[2mm] \dfrac{\partial p_z}{\partial d_1} & \dfrac{\partial p_z}{\partial \theta_2} & \dfrac{\partial p_z}{\partial \theta_3} & \dfrac{\partial p_z}{\partial \theta_4} & \dfrac{\partial p_z}{\partial d_5} & \dfrac{\partial p_z}{\partial \theta_6} \end{bmatrix} \tag{21}$$

Using (4) and (21),

$$\mathbf{J}_1 = \begin{bmatrix} 0 & \dfrac{\partial p_x}{\partial \theta_2} & \dfrac{\partial p_x}{\partial \theta_3} & C_{23}C_4(d_5+d_6) & C_{23}S_4 & 0 \\[2mm] 0 & 0 & 0 & S_4(d_5+d_6) & -C_4 & 0 \\[2mm] 1 & \dfrac{\partial p_z}{\partial \theta_2} & \dfrac{\partial p_z}{\partial \theta_3} & S_{23}C_4(d_5+d_6) & S_{23}S_4 & 0 \end{bmatrix} \tag{22}$$

where,

$$\frac{\partial p_x}{\partial \theta_2} = -a_2 S_2 - S_{23}(a_3 + S_4(d_5+d_6)) \quad \frac{\partial p_x}{\partial \theta_3} = -S_{23}(a_3 + S_4(d_5+d_6))$$

,   ,

$$\frac{\partial p_z}{\partial \theta_2} = a_2 C_2 + C_{23}(a_3 + S_4(d_5+d_6)) \quad \frac{\partial p_z}{\partial \theta_3} = C_{23}(a_3 + S_4(d_5+d_6))$$

,   .

$\mathbf{J}_2$ can be computed by using the rotation matrix $^0R_6$ and calculating

$w_6 = \begin{bmatrix} w_{6x} & w_{6y} & w_{6z} \end{bmatrix}^T$. Taking the time derivative of $^0R_6$ and multiplying the result with $^0R_6{}^{-1}$ will

result in a skew matrix.

$$\frac{\partial\,^0R_6}{\partial t}\,(^0R_6)^{-1} = \Omega \tag{23}$$

where,

$$\Omega = \begin{bmatrix} 0 & -w_{6z} & w_{6y} \\ w_{6z} & 0 & -w_{6x} \\ -w_{6y} & w_{6x} & 0 \end{bmatrix} \tag{24}$$

Using (4), (6), (23) and (24), angular velocity components of the end effector can be calculated as,

$w_{6x} = -S_{23}\dot{\theta}_4 + C_{23}S_4\dot{\theta}_6$, $w_{6y} = -\dot{\theta}_2 - \dot{\theta}_3 - C_4\dot{\theta}_6$, $w_{6z} = C_{23}\dot{\theta}_4 + S_{23}S_4\dot{\theta}_6$, and the second portion of the

Jacobian matrix $\mathbf{J}_2$ will be,

$$\mathbf{J}_2 = \begin{bmatrix} 0 & 0 & 0 & -S_{23} & 0 & C_{23}S_4 \\ 0 & -1 & -1 & 0 & 0 & -C_4 \\ 0 & 0 & 0 & C_{23} & 0 & S_{23}S_4 \end{bmatrix} \tag{25}$$

As the Jacobian matrix of the manipulator is known, from this point velocity analysis can easily be carried

out. Also by analyzing the Jacobian matrix, singular configurations of the manipulator can also be comput-

ed.

4.1 Direct and Inverse Velocity Problem

In the direct velocity analysis problem, the main objective is to calculate the linear and angular

velocities of the end effector by giving the actuated joint rates. As the Jacobian matrix is known, using (19)

the task can be easily carried out. In the inverse analysis problem, however; the main objective is to calcu-

late the actuated joint rates with respect to the known end effector velocity states. If (19) is pre multiplied

by the inverse of the Jacobian matrix, solution to the inverse velocity problem can easily be found as long

as the Jacobian inverse exist in other words, the matrix is nonsingular.

$$
\begin{bmatrix}
\dot{d}_1 \\
\dot{\theta}_2 \\
\dot{\theta}_3 \\
\dot{\theta}_4 \\
\dot{d}_5 \\
\dot{\theta}_6
\end{bmatrix}
= \mathbf{J}^{-1}
\begin{bmatrix}
v_6 \\
w_6
\end{bmatrix}
\tag{26}
$$

4.2 Singularity Analysis

As mentioned before, the inverse velocity problem, (26), can be solved as long as the inverse of

the Jacobian exists. On the other hand in some configurations of the manipulator, Jacobian matrix may

lose its full rank and become singular thus the numerical solution (26) will give infinite number of results

for the actuated joint rates.

In order to find those singular configurations, the determinant of the Jacobian matrix is equalized

to zero and solved for the variable joint parameters.

$$
\begin{aligned}
|\mathbf{J}| &= 0 \\
|\mathbf{J}| &= -S_2 S_4 C_4 a_2
\end{aligned}
\tag{27}
$$

Solving (27), reveals that the Jacobian matrix will be singular in the configurations where $\theta_2 = 0, \pi$ and

$$
\theta_4 = 0, \frac{\pi}{2}, \pi, \frac{3\pi}{2}.
$$

V. EXPERIMENTAL METHODS AND RESULTS

5.1 Measuring forces and results

Each angle of freedom was measured by using a force gage. Only wanted joint for measurement was checked in order to measure the force exclusively operated to each joint. When measuring Joint-1, arms are lined straight, and the end part of forceps is contacted to prove of force gage, where force gage is firmly fixed, using magnetic base. In order to measure rotational Joint-2, torque was measured with the surface of link 6cm away from the axis of rotation contacted to prove of force gage. For accurate measurement, link and prove are located exactly vertically such as figure 46. Measured value is divided by 6cm and converted to torque value. Measured were Joint-3, Joint-4 and Joint-5 like the way in Joint-1 and Joint-2. The every graph below each figure is results of each joint's torque and force. Every resultant value was higher than necessary except for Joint-3 which is driven by plate spring and Joint-4 which is driven by wires. In Joint-3 case, it can generate about 7N. Joint-4 can handle about 5N.
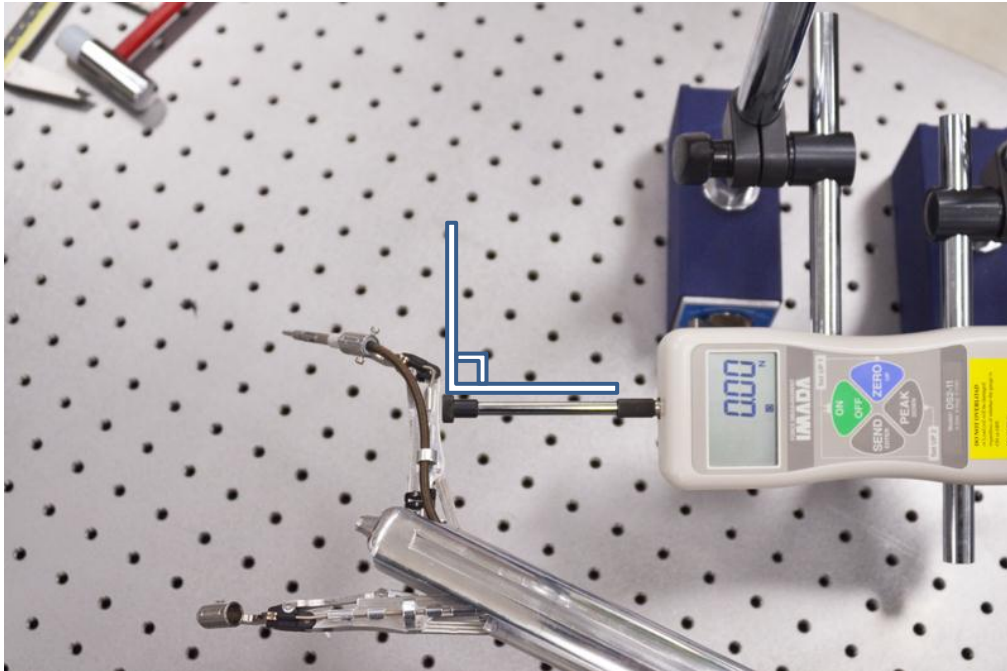
PLAS did not satisfy the required force of 10N but it could generate the most strong force among the already developed robotic SILS platforms.
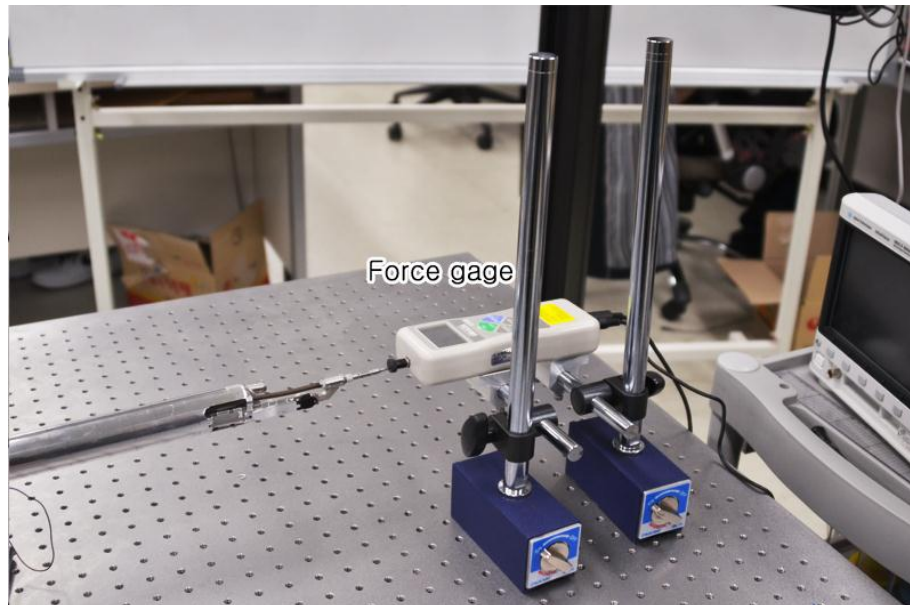
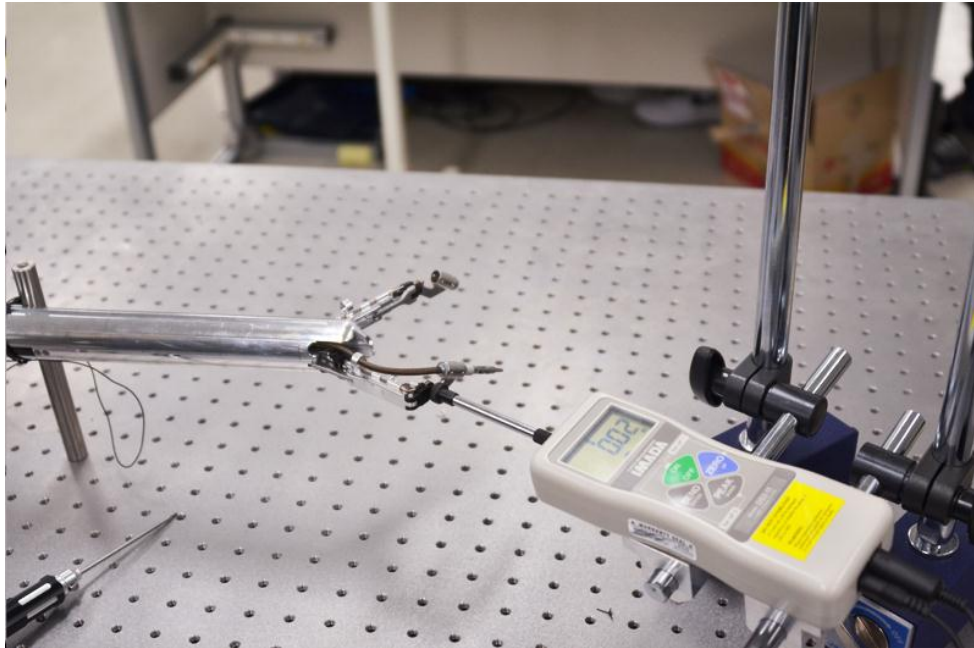**Figure 44.** The method of measuring Joint-1
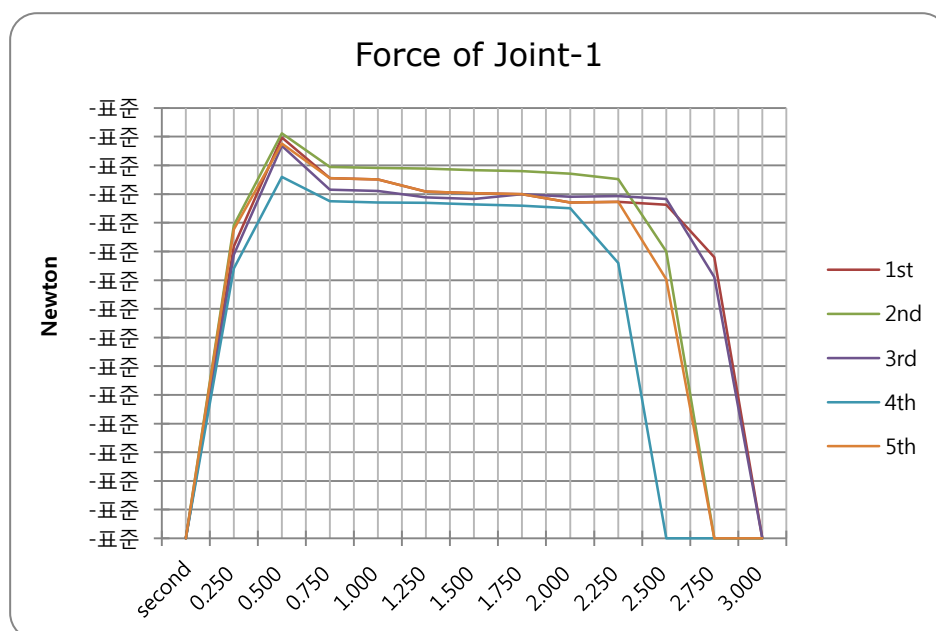
Figure 45. The result of measuring Joint-1

Figure 46. The method of measuring Joint 2

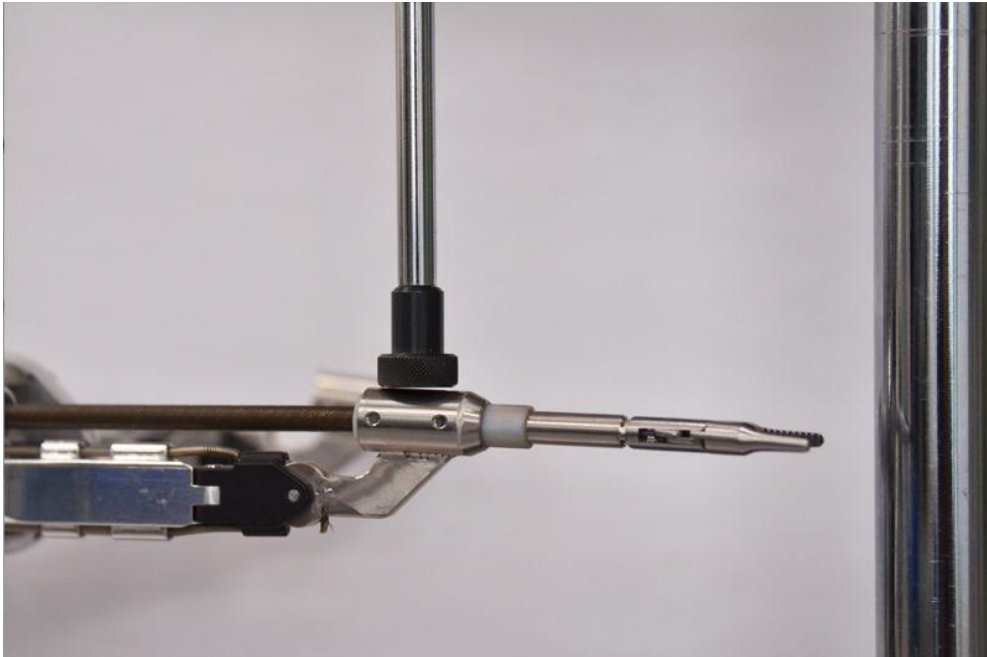**Figure 47.** The results of measuring Joint-2
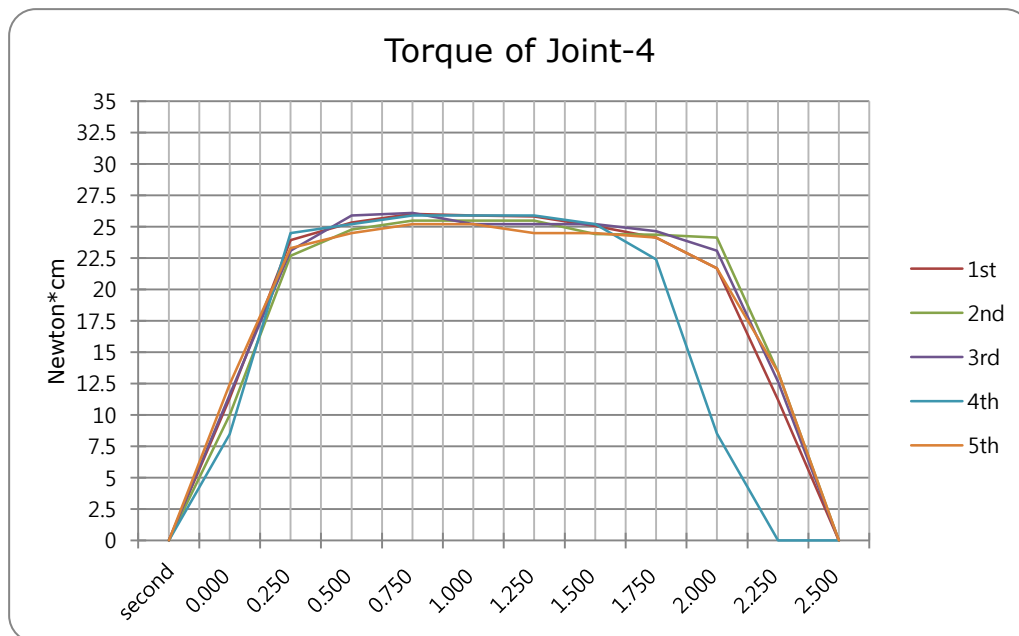
Figure 48. The method of measuring Joint 3

Figure 49. The result of measuring Joint-3
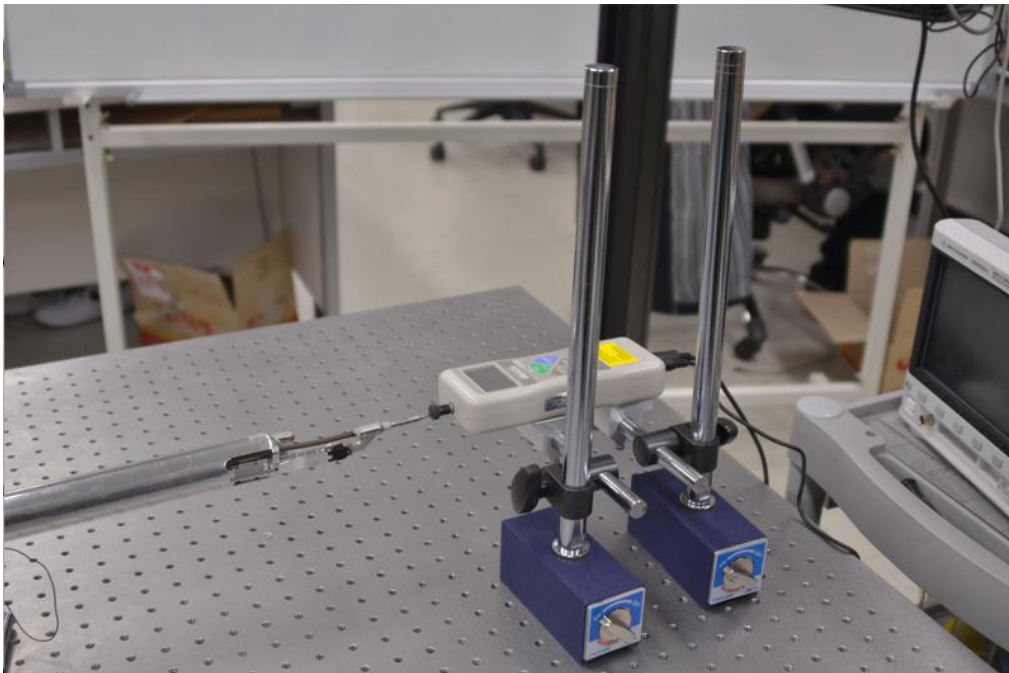
* The length between Joint-3 and an end effector: 7cm

Figure 50. The method of measuring Joint-4

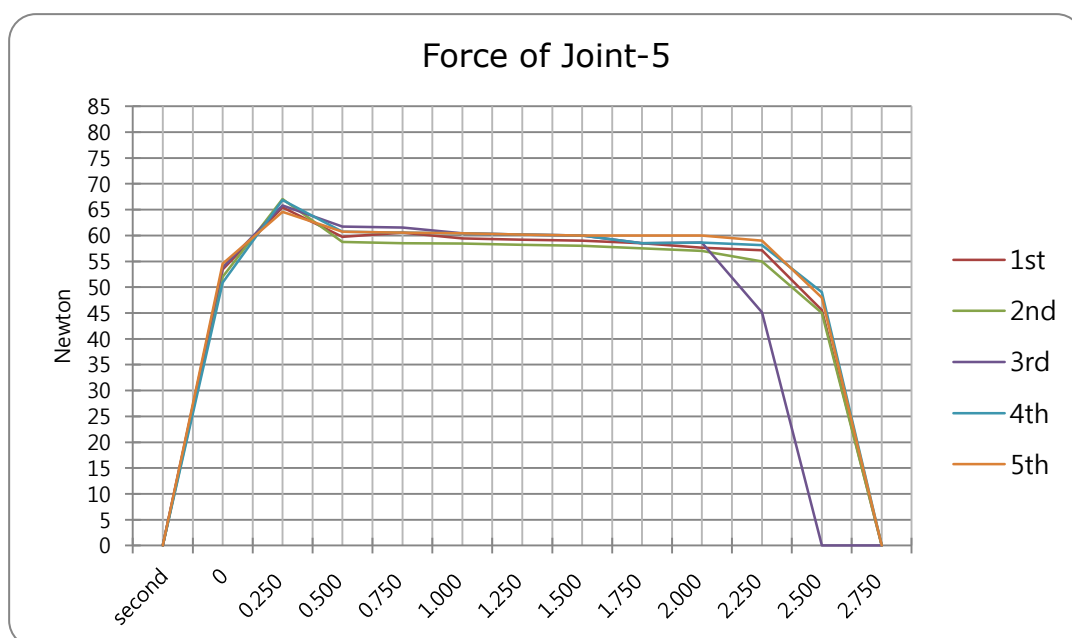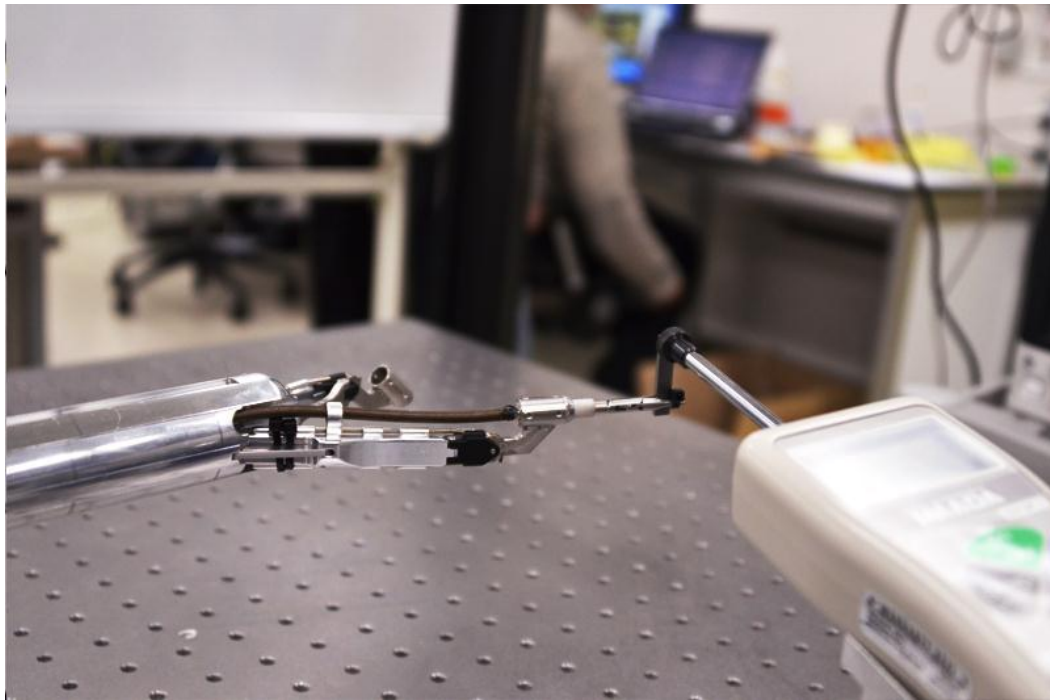**Figure 51.** The result of measuring Joint-4

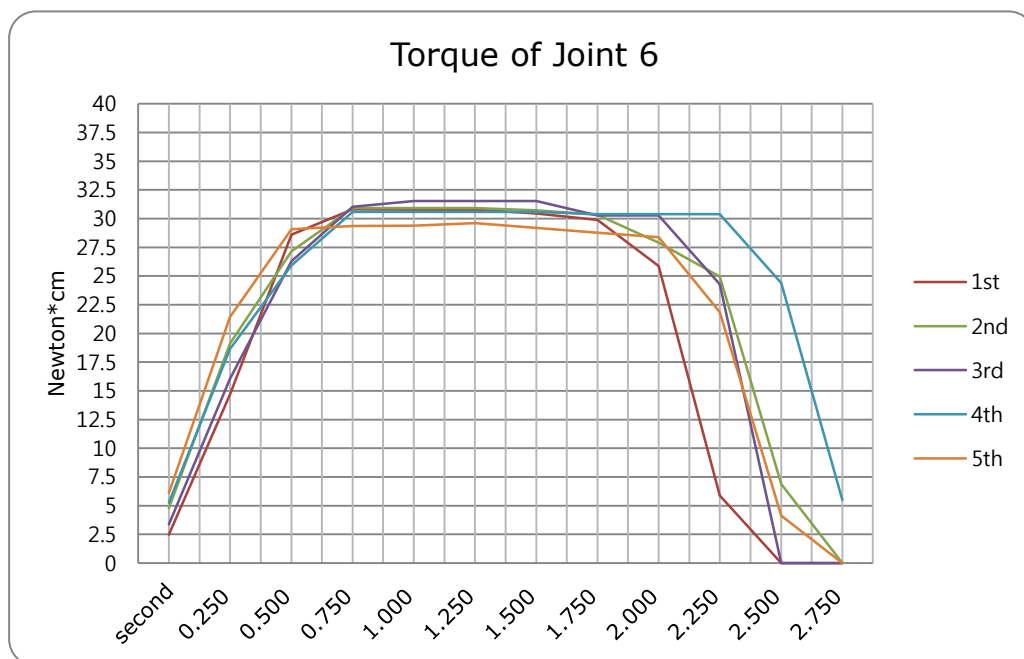* The length between Joint-4 and an end effector: 5cm
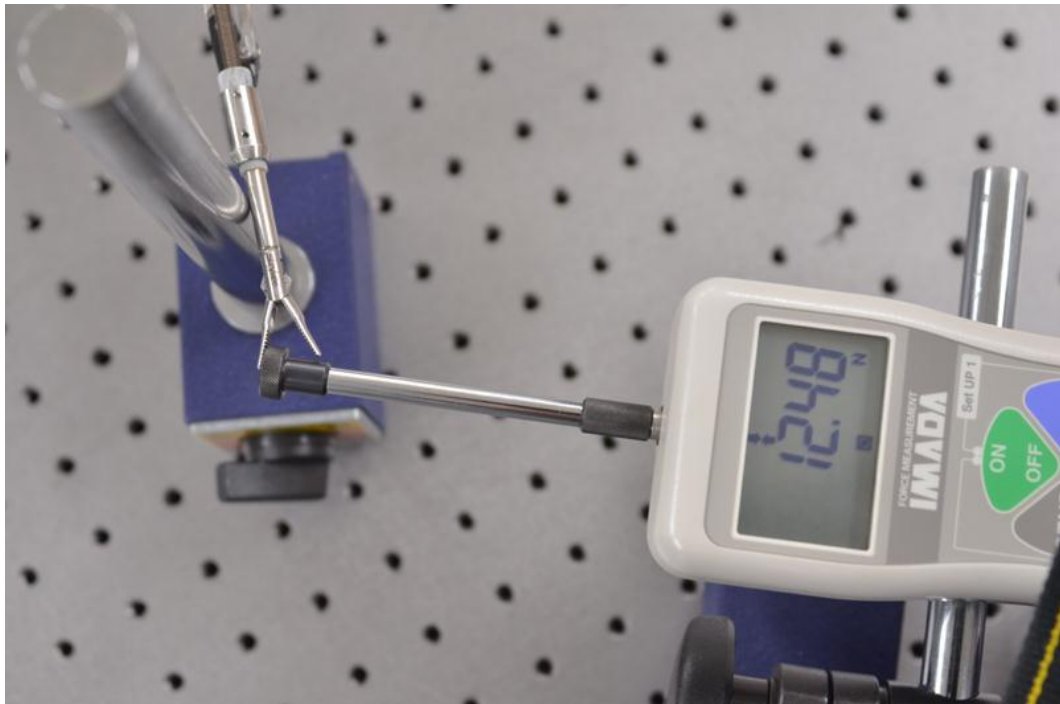
Figure 52. The method of measuring Joint 5

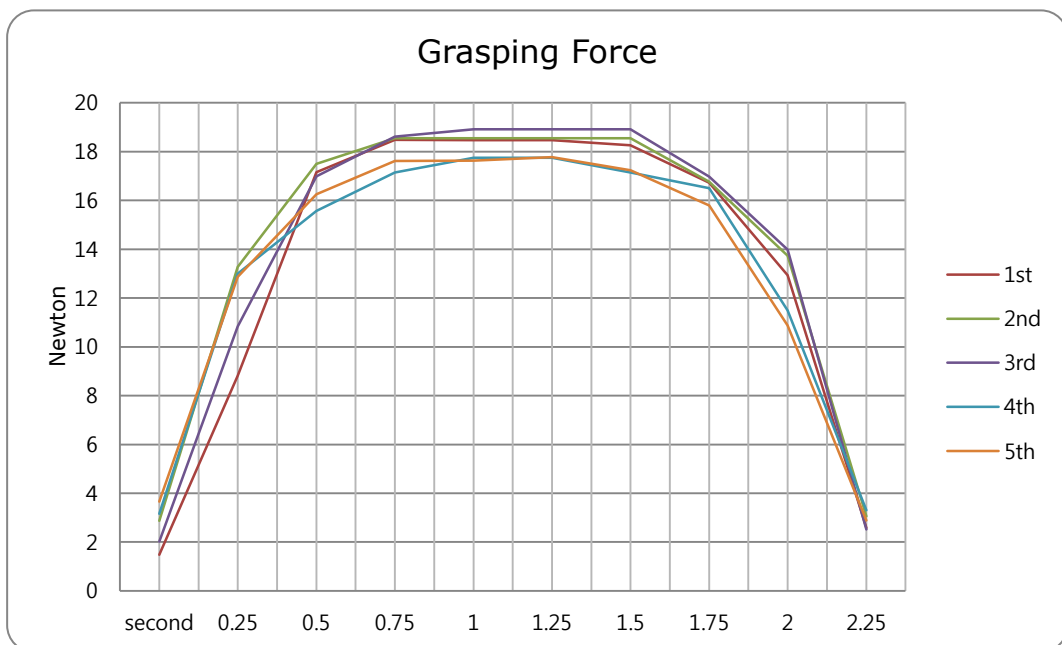**Figure 53.** The result of measuring Joint-5

Figure 54. The method of measuring Joint-6

**Figure 55.** The result of measuring Joint-6

Figure 56. The method of measuring grasping force

Figure 57. The result of measuring grasping force

5.2 Assessment for reliability of movements and its results

In order to measure reliability of movement by the difference of payload, the following experiment system was made. Located is Polaris Shown as figure 58 that draws out the location of infrared reflectors, and these reflectors are attached to the end of forceps. The goal of this study is to develop effective robotic SILS platform using plate spring driven mechanism, so only measured was Joint 3 that plate spring driven mechanism is applied to. At first, it is made to move 5 times repeatedly and identically at a state of payload '0', and in this trajectory was confirmed to be the same with the following graph. Afterwards, by increasing weight by 200g, 5 times of trial was measured. Experiment was measured and finished at the point when the robot could not move smoothly due to its weight. According to test results, every trajectory was uniform before weighing 1.6kg. This evaluation result has proved that the plate spring mechanism is suitable as a force delivery mechanism for surgery.
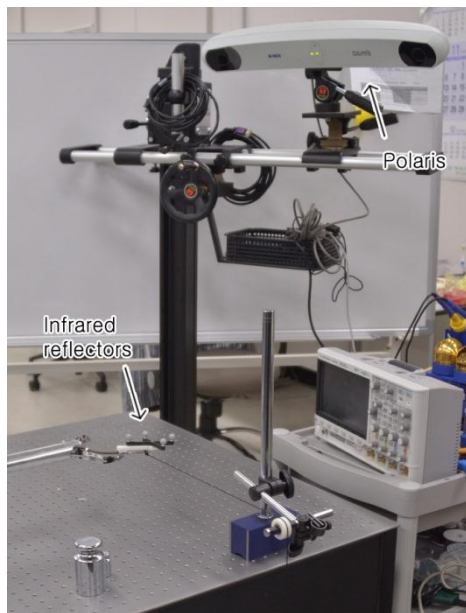
Figure 58. Polaris and infrared reflector
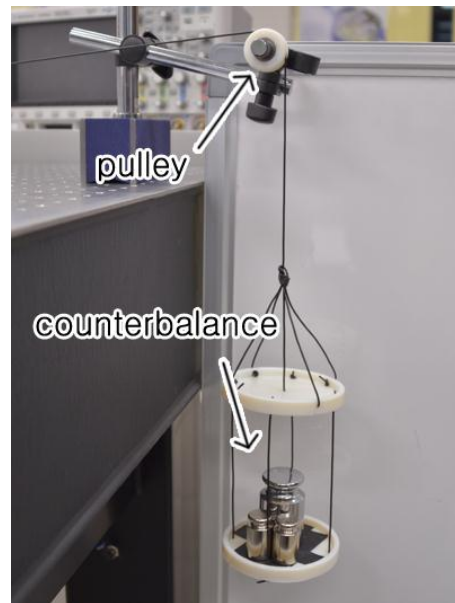
Figure 59. weight counteblance
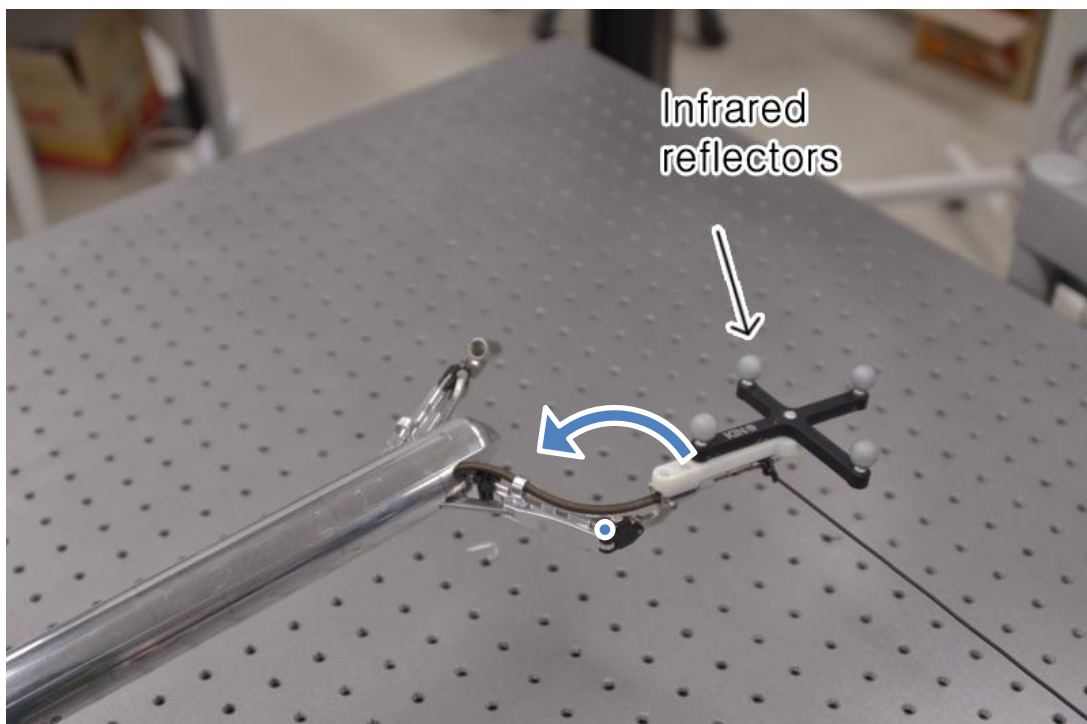
Figure 60. Direction of trajectory by Joint-3
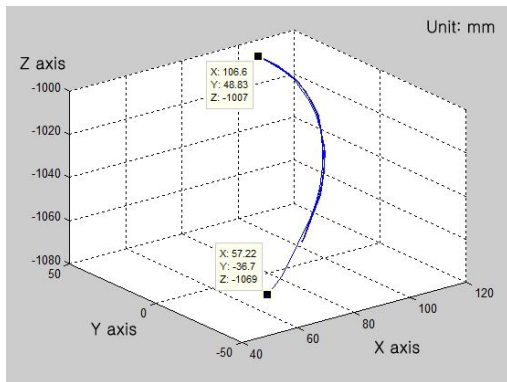
Figure 61. Trajectories of forceps (No load)
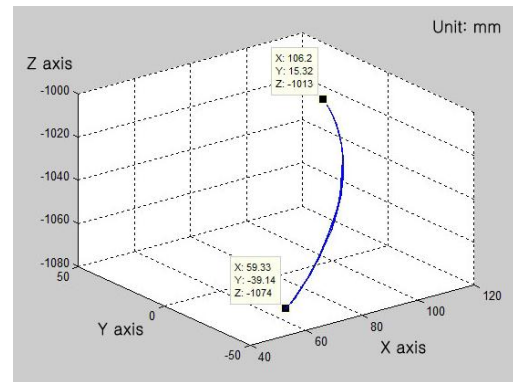
Figure 62. Trajectories of forceps (payload=200g)
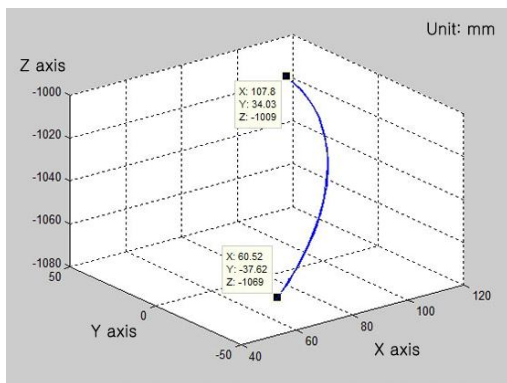
Figure 63. Trajectories of forceps (payload=400g)
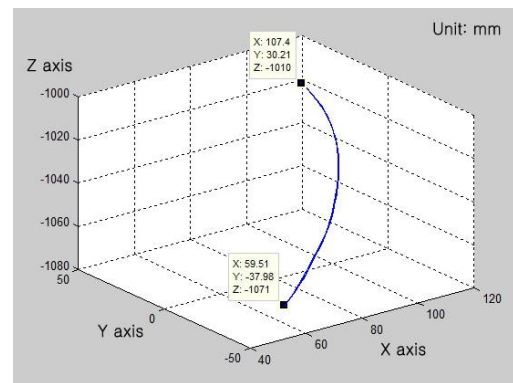
Figure 64. Trajectories of forceps (payload=600g)
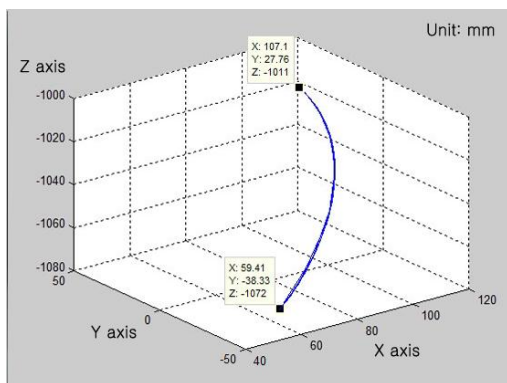
Figure 65. Trajectories of forceps (payload=800g)
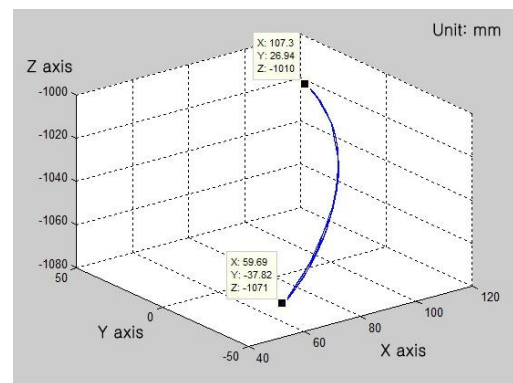
Figure 66. Trajectories of forceps (payload=1200g)
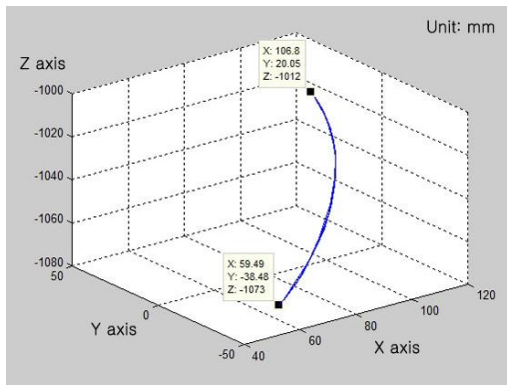
Figure 67. Trajectories of forceps (payload=1400g)   **Figure 68.** Trajectories of forceps (payload=1600g)
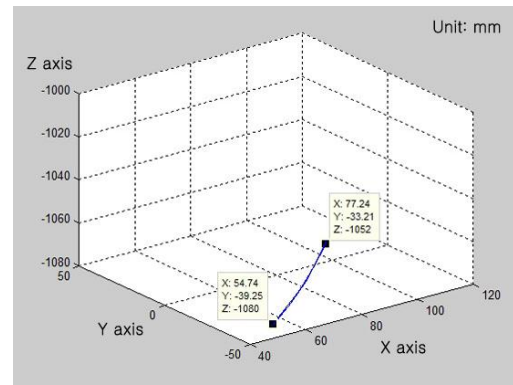
VI. CONCLUSION AND FURTHER WORKS

In this paper, the performances of PLAS have been assessed, designing and realizing a single port surgery robot, attached with plate spring mechanism, a new form of device of delivering force. Based on deep understanding of a single port surgery, the goal of this paper is to develop an effective robotic SILS platform. In order to achieve this goal, developed was effective robotic SILS platform that conducts the single port surgery after taking advantages and solving weaknesses of existing robotic SILS platform in cooperation with surgeons.

First, SILS was reviewed so as to develop a robotic SILS platform. Difficulties that surgeons face were analyzed, observing surgeons operating and solutions about existing robots were looked through to breakthrough this hardship. By this process, solutions were suggested, drawing out weaknesses that existing SILS robotic platforms have. The first problem derives from limits of force-delivering device that existing SILS robots adopt. Due to the lack of stiffness of wires, robots that use wire driven mechanism for delivering force cannot afford enough force, and gear-using-robots cannot be inserted to a small port owing to its large volume, which is caused by the size of mechanical gears. In this study, a new way of delivering force that has not been introduced before was applied to solve this problem. This is a way, using

plate spring, in which a structure and principle are simple, and has an advantage of delivering relatively big force for its volume. The minimization of operating robots is required especially in a trend that minimal invasive operations spread, and plate spring mechanism as a force delivering device is being conformed to be effective through this experiment.

The second problem is that current robots which are used to solve counter intuitive operation problem cannot deal with relatively large sized intestine. This problem originates from the fact that the arm of the robot is fixed at a point when the arm spreads with a shape of 'Y'; Y-shaped-robots are supposed to have a short stroke. Operations that are possible by manual SILS are not possible in SILS robots that are meant to have operations easy. This study enables this problem to be solved by installing slide link at a point where the arm is spread to 'Y' shape. Operations for stomach, small intestine and large intestine which need a long stroke are expected to be feasible with a robot that has a new 'Y' shape form.

Suggested are realistic potential and examples that ideal robotic SILS platform can accomplish, securing the length of stroke that the conventional laparoscopic surgery has, solving the biggest problem of single port operating robot - a force delivery.

It is when surgeons constantly use the robot in a real operation circumstance that the most effec-

tive feedback can appear. In this study, surgeons' opinions are just taken into consideration. However, surgeons who use robots in operations were not made to participate in applying it to a real operation. In order to finalize the development of operating robots, needed is a process where surgeons apply it into a real situation and assess its results. Moreover, following factors should be managed. Easiness of exchanging surgical instruments and optimization of selecting motors should be fully met. Also, wire driven mechanism should be exchanged to a way that stiffness is satisfied, considering a tilting joint that delivers force by wires in the proposed robot. Besides, the size of the robot body should be minimized within 30mm by processing the robot's body frame with stainless steel. In order for this process to be possible, reduction in a process cost should be needed. Along with this, robots should be designed to be a structure where strong stainless steel can be easily processed. If these problems should be solved, the single port surgery robot would be expected to be used as widely as the da Vinci surgical system.

References

[1] MD Woo-Jung Lee. (2010) "Single port laparoscopic surgery" Journal of the Korean Medical Association, 53 (9) pp. 793-806.

[2] M. T. Gettman, Y. Lotan, C. A. Napper and J. A. Cadeddu. (2002) Mar. "Transvaginal laparoscopic nephrectomy: development and feasibility in the porcine model," Urology, 59 (3) pp. 446-450.

[3] R. V. Clayman, G. N. Box, J. B. Abraham, et al. (2007) Jun. "Rapid communication: transvaginal single-port NOTES nephrectomy: initial laboratory experience," Journal of Endourology, 21 (6) pp. 640-644.

[4] E. Lima, C. Rolanda, J. M. Pego, et al. (2007) Dec. "Third-generation nephrectomy by natural orifice transluminal endoscopic surgery," Journal of Urology, 178 (6) pp. 2648-2654.

[5] R. Autorino, J. A. Cadeddu, M. M. Desai, et al. (2011) Jan. "Laparoendoscopic single-site and natural orifice transluminal endoscopic surgery in urology: a critical analysis of the literature," European Urology, 59 (1) pp. 26-45.

[6] J. D. Raman, J. A. Cadeddu, P. Rao and A. Rane. (2008) Jun. "Single-incision laparoscopic surgery: initial urological experience and comparison with natural-orifice transluminal endoscopic surgery," British Journal of Urology International, 101 (12) pp. 1493-1496.

[7] C. Esposito. (1998) Feb. "One-trocar appendectomy in pediatric surgery," Surgical Endoscopy, 12 (2) pp. 177-178.

[8] P. W. Dhumane, M. Diana, J. Leroy and J. Marescaux. (2011) Jan. "Minimally invasive single-site surgery for the digestive system: A technological review," Journal of minimal access surgery, 7 (1) pp. 40-51.

[9] R. Autorino, R. J. Stein, E. Lima, et al. (2010) May. "Current status and future perspectives in laparoendoscopic single-site and natural orifice transluminal endoscopic urological surgery," International Journal of Urology, 17 (5) pp. 410-431.

[10] J. H. Kaouk and R. K. Goel. (2009) May. "Single-port laparoscopic and robotic partial nephrectomy," European Urology, 55 (5) pp. 1163-1169.

[11] M. T. Gettman, W. M. White, M. Aron, et al. (2011) Feb. "Where do we really stand with LESS and NOTES?," European Urology, 59 (2) pp. 231-234.

[12] J. H. Kaouk, R. K. Goel, G. P. Haber, S. Crouzet and R. J. Stein. (2009) Feb"Robotic single-port transumbilical surgery in humans: initial report," British Journal of Urology International, 103 (3) pp. 366-369.

[13] Autorino R, Cadeddu JA, Desai MM, et al. (2011) "Laparoendoscopic single site and natural orifice transluminal endoscopic surgery in urology: a critical analysis of the literature," European Urology, (59) pp. 26-45.

[14] L. Cindolo, S. Gidaro, F. R. Tamburro and L. Schips. (2010) May. "Laparo-endoscopic single-site left transperitoneal adrenalectomy," European Urology, 57 (5) pp. 911-914.

[15] R. Autorino, J. H. Kaouk, J. U. Stolzenburg, et al. (2012) Aug. "Current Status and Future Directions of Robotic Single-Site Surgery: A Systematic Review," European Urology

[16] Y. Horise, A. Nishikawa, M. Sekimoto, et al. (2012) Mar. "Development and evaluation of a master-slave robot system for single-incision laparoscopic surgery," International Journal of Computer Assisted Radiology and Surgery, 7 (2) pp. 289-296.

[17] G. P. Haber, R. Autorino, H. Laydner, et al. (2012) Feb. "SPIDER surgical system for urologic procedures with laparoendoscopic single-site surgery: from initial laboratory experience to first clinical application," European Urology, 61 (2) pp. 415-422.

[18] Kai Xu, Roger E. Goldman, Jienan Ding, Peter K. Allen, Dennis L. Fowler and Nabil Simaa. (2009) Oct. "System Design of an Insertable Robotic Effector Platform for Single Port Access (SPA) Surgery," Intelligent Robots and Systems, pp. 5546-5552.

[19] Marco Piccigallo, Umberto Scarfogliero, Claudio Quaglia, Gianluigi Petroni, Pietro Valdastri, Arianna Menciassi, and Paolo Dario. (2010) "Design of a Novel Bimanual Robotic System for Single-Port Laparoscopy," IEEE/ASME Transactions on Mechatronics, 15

[20] Hoyul Lee, Youngjin Choi, and Byung-Ju Yi. (2012) "Stackable 4-BAR Manipulators for Single Port Access Surgery," IEEE/ASME Transactions on Mechatronics, 17 (1),

[21] Y. Kobayashi, Y. Tomono, Y. Sekiguchi, et al. (2010) Dec. "A surgical robot with vision field control for single port endoscopic surgery," International Journal of Medical Robotics and Computer Assisted Surgery, 6 (4) pp. 454-464.

[22] Y. Sekiguchi, Y. Kobayashi, H. Watanabe, et al. (2011) "In vivo experiments of a surgical robot with vision field control for Single Port Endoscopic Surgery," Engineering in Medicine and Biology Society, Annual International Conference of the IEEE, pp. 7045-7048.

[23] C. Richards, J. Rosen, B. Hannaford, C. Pellegrini, M. Sinanan (2000) Aug. "Skills evaluation in minimally invasive surgery using force/torque signatures," Surgical Endoscopy, (14) pp. 791–798

[24] M. Lazeroms, G. Villavicencio, W. Jongkind, and G. Honderd, (1996) "Optical fibre force sensor for minimal-invasive-surgery grasping instruments," Engineering in Medicine and Biology Society, Bridging Disciplines for Biomedicine. Proceedings of the 18th Annual International Conference of the IEEE, (1).

요 약 문

본 연구에서는 판 스프링을 구동 메커니즘으로 하는 새로운 형태의 단일공복강경 수술 로봇을 개발하였다.

최근, 복부에 3~5 개의 상처를 남기는 기존의 복강경 수술의 대안으로 수술 후 상처를 쉽게 숨길 수 있는 배꼽을

통한 단일 공 복강경 수술(single port laparoscopic surgery)의 수요가 증가하는 추세이다. 하지만 단일 공 복강경

수술은 내시경과 두 개의 겸자(forceps)가 단 하나의 침습 구로 삽입되어 시술 중 도구간의 충돌을 피하기

어려우며, 작업 공간을 확보하기도 힘들다. 이러한 문제를 해결하기 위해 여러 가지 단일 공 복강경 수술 로봇이

개발 되고 있지만 수술을 하기에 충분한 힘을 전달하지 못하는 문제가 있다. 이 논문에서는 위와 같은 문제를

해결하고, 수술에 필요한 충분한 힘과 넓은 작업영역을 확보하기 위해 판 스프링으로 구동되는 단일

공 수술로봇을 설계, 제작한 후 성능평가를 실시했다.

국내에서는 처음 개발되는 Y 타입 단일 공 수술로봇을 개발하기 위해 매뉴얼 단일 공 복강경

수술의 임상적인 제한 사항과 기존에 개발된 단일 공 복강경 수술로봇의 장단점을 심도 있게

분석하여 기구 설계에 적용시켰다. 특히 의사들의 현장 경험과 의견을 수용하여 기구설계에 적극

반영하였으며, 기존 단일 공 수술 로봇들보다 넓은 작업공간을 갖는 단일 공 수술 로봇을 개발할 수

있었다.

ACKNOWLEDGEMENT

얻어 마셨던 와인 한 잔 따라드릴 수 있는 한결 같은 제자가 되도록 하겠습니다.

항상 부족한 신입 직원을 위해 덕담을 아끼지 않으셨던 정 많으신 정성택 부장님, 한참 부서가 어려울 때 세상 무서운지 모르고 퇴직 한하고 힘들게 해드렸는데, 오랜 시간이 흘렀어도 잊지 않으시고 취업자리까지 챙겨주시고 진심으로 감사 드립니다. 저를 더 큰 세상으로 인도해주시고 멘토 역할을 해주신 김성주 차장님. 딱딱한 회사 생활 속에서 여러 가지 즐거운 추억들을 함께 만들어 주셔서 감사합니다. 그리고 차장님 계실 때 로봇 대회 우승 못한 것 너무 죄송합니다.

교고 시절 목표를 갖고 최선을 다하는 것이 무엇인지 알려주신 구연욱 선생님, 선생님과 함께 한 시간 때문에 제가 많이 변했고 생각도 없었던 대학까지 갈 수 있었습니다. 진심으로 감사 드립니다.

광현이와 용철이, 너희는 내게 천재이고 든든한 팀원이었다. 너희 때문에 로봇 팀 생활이 분에 넘치게 영광스러웠다. 정말 고마웠다. 앞으로도 지금처럼 서로 챙겨주고 도우면서 살아가자. 로봇 팀 생활하며 고생 많이 한 옥진이, 지우, 현아 그리고 힘들고 반복적인 일도 즐겁게 해준 귀택이 수고 많이 했고 너희 때문에 로봇 팀 생활도 즐거웠다. 마지막 휴머노이드 로봇 팀장 수철이와 동현이, 창훈이, 민정이, 혜민이, 협이 너희들은 너희 로봇 팀 생활이 어떻게 기억 될지 모르겠지만 내게는 참 대견했고, 소중한 마지막 로봇 팀이었다. 최선을 다해 마지막을 준비해준 열정에 진심으로 고맙다.

회사 출근 하시기 전에 새벽 네 시에 두 달 동안 공업수학 수업 해주신 택근이형 진심으로 감사 드립니다. 저도 무척 힘들었지만 형님도 정말 수고가 많으셨습니다. 꼭 좋은 논문 많이 쓰셔서 한기대 교수로 돌아 오시길 빕니다. 우제영감, 내가 회사 다닐 때 새벽 3 시에도 전화를 받아줘서 독서실에서 집으로 돌아가는 길이 외롭지 않았는데 참 고마웠어. 그리고 그렇게 열심히 도와줬는데 카이스트 떨어져서 미안했어. 그리고 취업자리 추천해줘서 정말 고마워. 경민아 너 때문에 카이스트 낙방하고 버틸 수 있었다. 그리고 너의 물심양면의 지원이 없었다면 학교 앞에서 자취할 때 무척이나 고생 많이 했을 텐데. 정말 고맙다. 너의 투자가 빛을 보도록 열심히 살게. 한철아 너 때문에 학부 때 로봇팀장도 하면서 랩장을 무사히 마칠 수 있었어, 또 회사 다닐 때 외로운 서울 생활을 잘 버틸 수 있었다. 사실 네가 대학원 생활하며 밥 사달라고 하고 책 사달라고 했을 때 네게 도움을 줄 수 있어서 내 스스로에게도 뿌듯했다. 그리고 왕 언니 지연아 항상 진심으로 대해주고 걱정해줘서 고마웠어.

마지막으로 어려운 가정 환경 속에서 공부에만 전념 할 수 있게 해주신 부모님 감사 드립니다. 회사를 그만두고 나와 속 썩혀드린 것 죄송하고, 부모님도 저의 석사 생활 동안 수고 많이 하셨습니다. 그 동안 효도 못해드린 만큼 앞으로 더욱 효도 하겠습니다. 병주야 늦은 밤에 영작 질문 해도 바로 바로 알려줘서 논문 쓰는데 정말 큰 도움이 됐어 정말 고마워. 준서야, 혜원아 큰 형, 오빠로서 항상 역할을 못해서 미안해. 부모님에게 자랑스러운 자식이 될 수 있도록 열심히 살자.

<div align="right">

2013. 12. 31.

천병식

</div>

APPENDIX

A. Specification of Force Gage

- Manufacturer: IMADA

- Model: DS2-50N

| Accuracy:	± 0.2% Full scale ± 1 LSD
Display:	4 digit, 12 mm high
Range	0~ 50N (5kgf)
Overload capacity:	200% Full scale, display flashes beyond 105% full scale
Data Processing Speed	1,000 data/second (30 data/second rate selectable)
Display Update	10 times per second
Outputs	RS-232, Mitutoyo Digimatic and ±1 VDC analog output
Temperature range:	32° to 100° F (0 - 40° C)
Low battery indicator:	Display flashes when battery is low
Power supply:	Rechargeable NiMH battery pack or AC adapter (included)
Setpoints	Programmable high/low setpoints with LCD indicators
Housing dimension:	215 x 65 x 51 mm (L x W x H)
Weight, net (gross)	approx. 430 g (1300 g)
Warranty	2 Years

B. Specification of Servo motor

- Manufacturer: Robotis

Model	MX-64R		
Weight	126g		
Dimension	40.2mm x 61.1mm x 41mm		
Gear ratio	200:01:00		
Operation Voltage (V)	11	12	14.8
Stall Torque (N.m)	5.5	6	7.3
Stall Current (A)	3.9	4.1	5.2
No Load Speed (RPM)	58	63	78
Motor	Maxon Motor		
Resolution	약 0.088° x 4,096		
Range	360°		
Voltage	10~14.8V (Recommended voltage : 12V)		
Operating temperature	-5°C ~ 80°C		
Communication Type	Digital Packet		
Protocol	RS485 Asynchronous Serial Communication		
Link (physical)	RS485 Multi Drop Bus (daisy chain type connector)		
ID	254 ID (0~253)		
Communication speed	8000bps ~ 4.5Mbps		
Feed back	Position, Temperature, Load, Input Voltage, Current, etc.		
Encoder	Contactless absolute encoder		

C. Specification of Stepping motor

- Manufacturer: MASURU
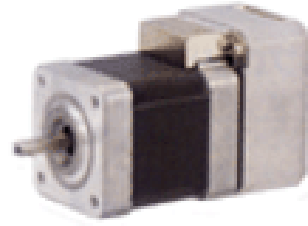
Model	CM1-17L30A
Output Power	18W
RPM	3000rpm
Torque	3.7(0.38) kgfcm(Nm)
Peak Torque	5.3(0.54) kgfcm(Nm)
Encoder	Incremental magnetic (50000pulses/rev)
Control type	Closed Loop
Voltage	V DC24V 10%
Current	A 1.5A / 1.8A
Pulse/Rev	200, 400, 500, 1000(default), 2000, 2500, 5000, 10000, 25000, 50000
Weight	470g

Curriculum Vitae

Name: Byungsik Cheon
Birth Date: July 8th 1979

Education

1999-2007   Korea University of Technology and Education.
            Mechatronics Engineering

Work Experience

2007-2009   KT, Central Research and Development Center.
            Researcher

Professional Activities

Project Manager of
Public Relations and Guide ROBOT Business Model Development based on URC

Honors and Awards

Cap-Stone Design Award 2006, Grand prize, Prime Minister's Prize
International robot contest 2006, All-round Championship, President's Prize
International robot contest 2008, Individual Championship, Minister's prize
Korea-Japan robot grand prix. 2006, the 1st Prize